

Strengthening of Metallic Members using CFRP Materials

Hossein Heydarinouri

Dr. sc. EPFL, Lausanne
Empa, Swiss Federal Laboratories for Materials Science and Technology
Überlandstrasse 129, 8600 Dübendorf, Switzerland
Tel: +41 58 765 4192 / Mobile: +41 78 235 77 10
E-Mail: hossein.heydarinouri@empa.ch

Outlines

- Introduction & Motivation
- Flexural Strengthening
- Lateral Torsional Buckling (LTB) Strengthening
- Fatigue Strengthening of Healthy Metallic Members
- Case Studies:
 - ✓ Fatigue Strengthening of Münchenstein Railway Bridge **Girders**
 - ✓ Fatigue Strengthening of Aabach Railway Bridge **Connections**

Introduction

Market:

Europe:

- 22% bridges are metallic
- 70% are older than 50 years

Switzerland:

- Swiss Federal Railways (SBB) has 6050 railway bridges
- 25% of bridges older than 80 years are metallic riveted

Problems in Metallic Bridges:

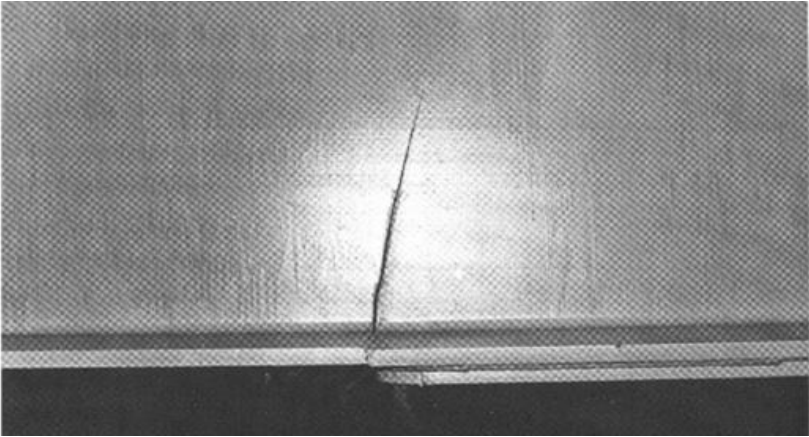
- Insufficient fatigue crack safety
- Need for upgrade to carry larger loads/traffic
- Most commonly used structural metals:
Steel, wrought irons, cast irons



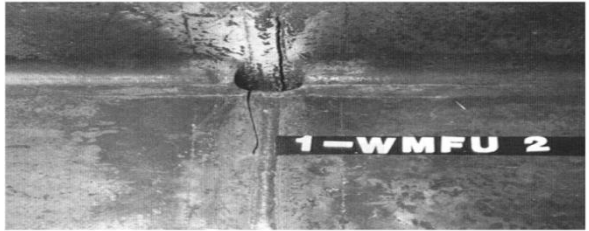
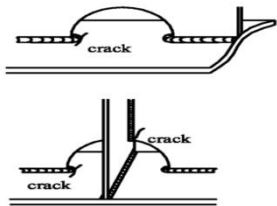
Chajes et al. „Fracture: Field testing of the I-95 bridge.“ In Third Annual Bridge Workshop: Fatigue and Fracture; Center of Innovative Bridge Engineering: Ames, IA,USA, 2004



Introduction



Kuehn et al. „Assessment of Existing Steel Structures: Recommendations for Estimation of Remaining Fatigue Life“; the Publications Office of the European Union: Luxembourg, 2008



Kuehn et al. „Assessment of Existing Steel Structures: Recommendations for Estimation of Remaining Fatigue Life“; the Publications Office of the European Union: Luxembourg, 2008



Fisher, J.W. “Fatigue and Fracture in Steel Bridges”; Wiley-Interscience: Hoboken, USA, 1984



Daniel Hoan Memorial Bridge, Milwaukee, Wisconsin, Failure on the 13th of December 2000



Examples of fatigue cracked bridges



Photos taken by Elyas Ghafoori, April. 2017



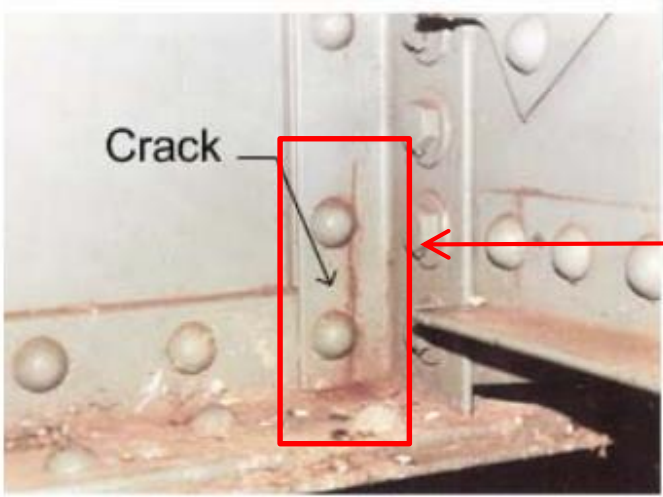
Steel Strengthening

Fibre Composites

Hossein Heydarinouri

6

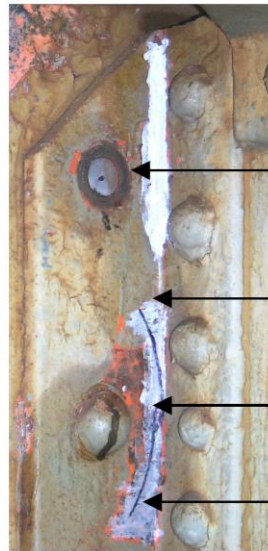
Examples of fatigue cracked bridges



Rivet failure: rivet head pop-out



Rivet failure: rivet head pop-out



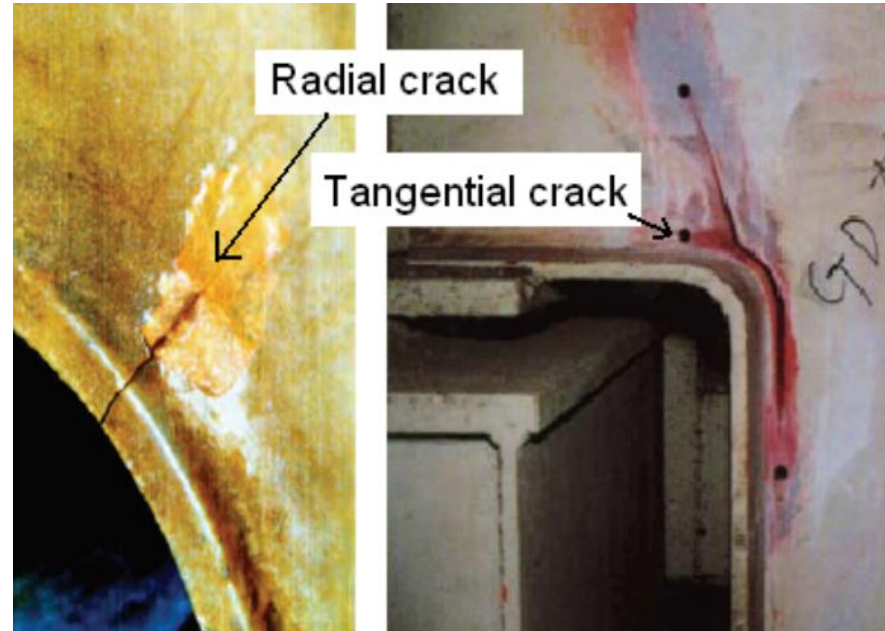
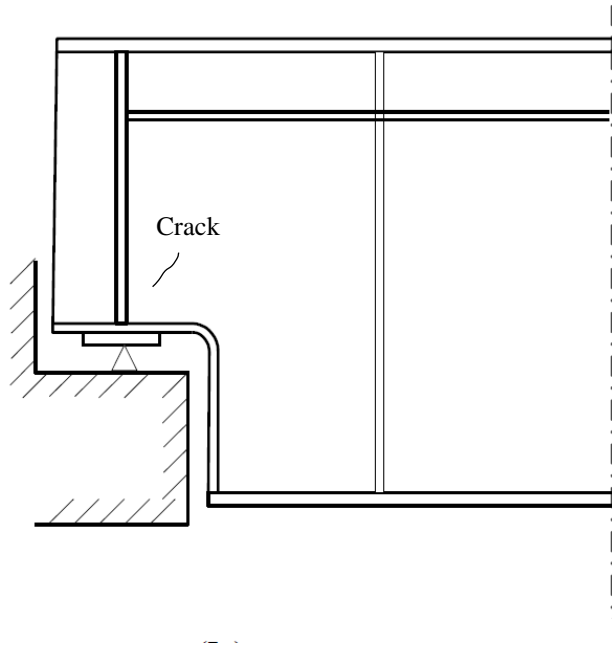
Rivet failure: rivet head pop-out

Crack propagation

Crack initiation in the fillet

Crack propagation

Typical fatigue cracks that can be found near supports of metallic girders (due to change of stiffness) in metallic bridges

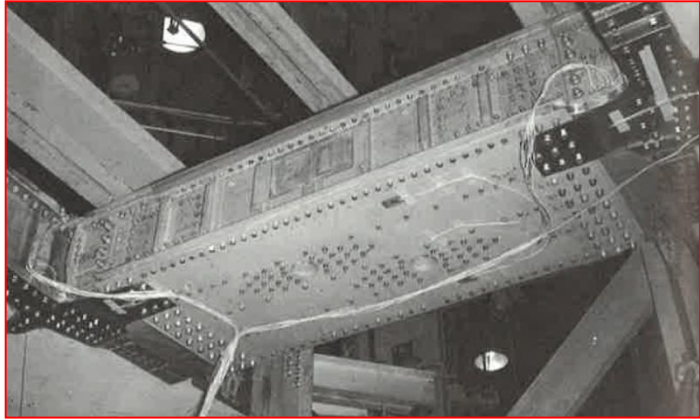


A metallic bridge in Sweden

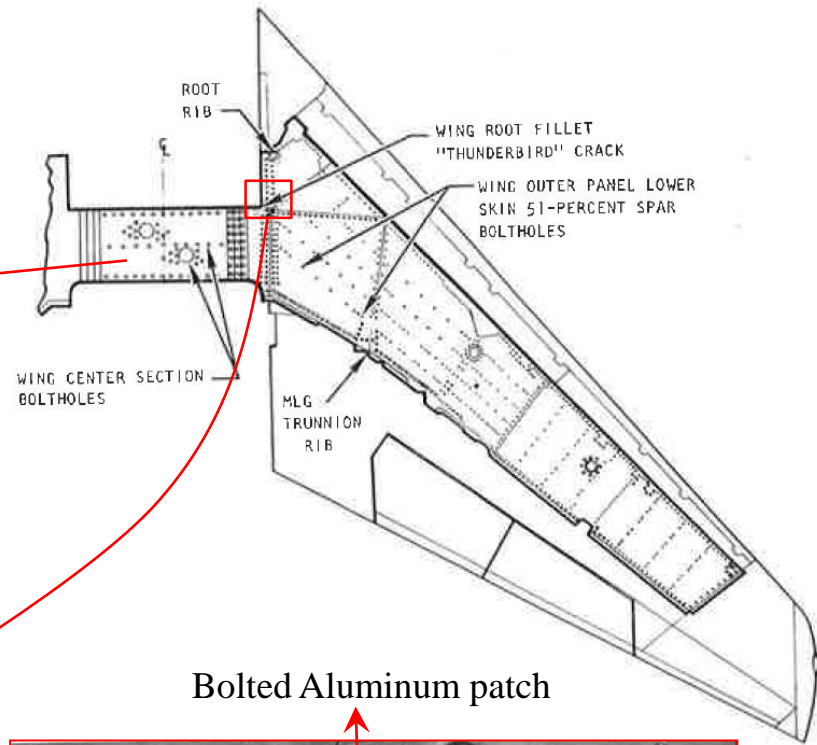
Introduction

Retrofit of metallic aircrafts

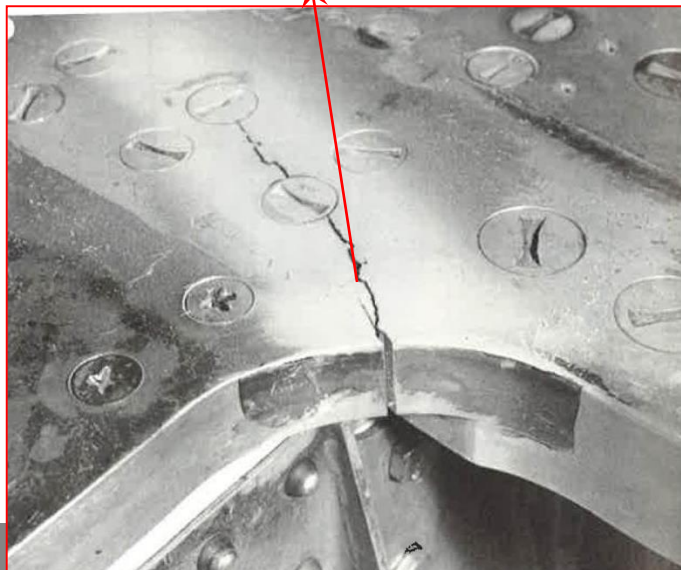
Retrofit of F-100 wing structure



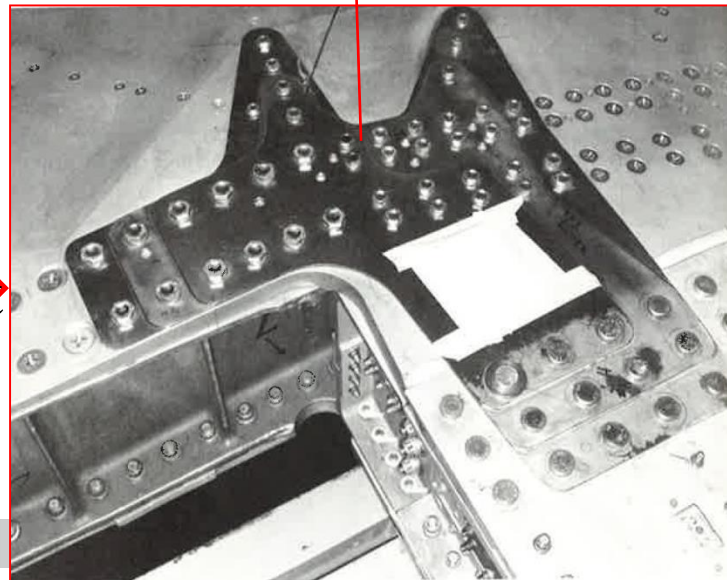
Fatigue crack in wing root fillet



Bolted Aluminum patch



Retrofit

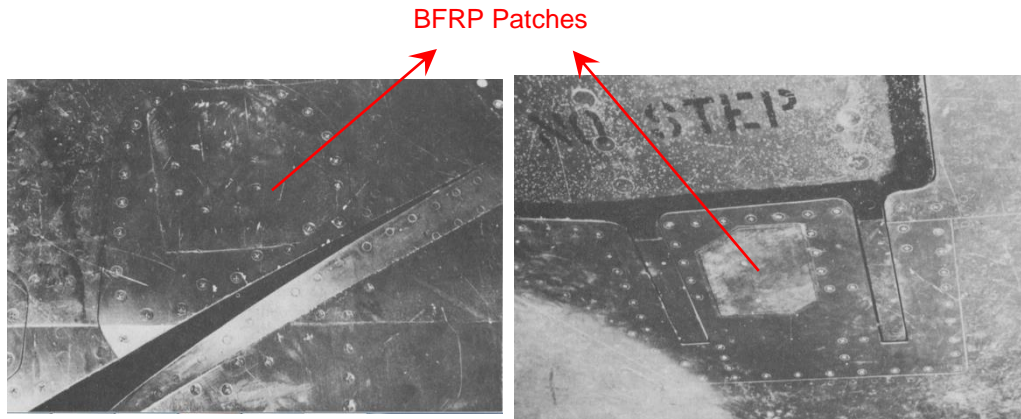


re Composites

hour

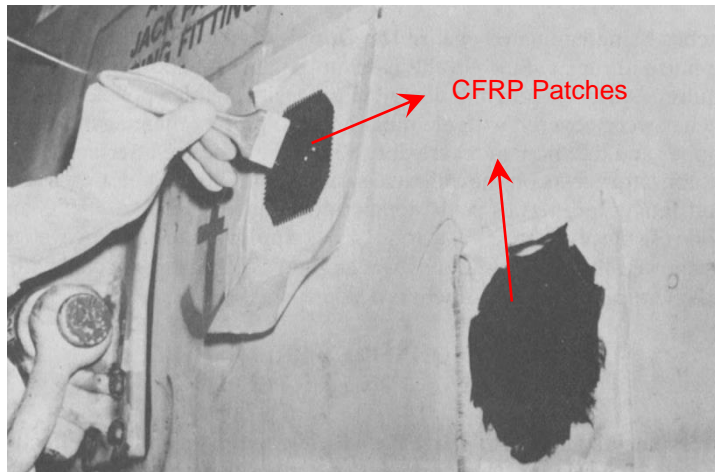
Introduction

Retrofitting of aircrafts with bonded composite materials

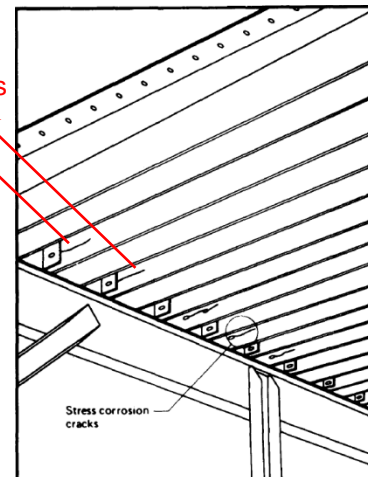


BFRP patch bonded to the wing skin of a Mirage aircraft

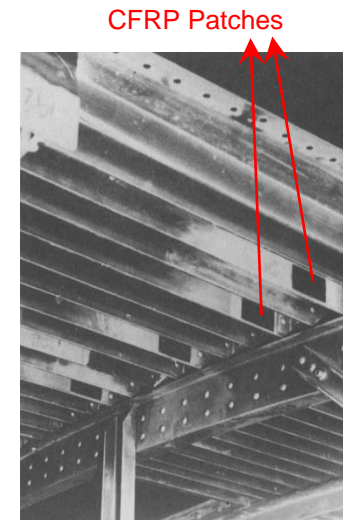
CFRP patch bonded to the fuselage of an Orion aircraft



CFRP Patches



Schematic view of the underside of a Hercules upper wing plank showing location of typical stress-corrosion cracks.



Cracking	Material	Component	Aircraft	Comments
Stress-corrosion	7075T6	Wing plank ^a	Hercules	Over 300 repairs since 1975
Fatigue	Mg Alloy MSR	Landing wheel ^d	Macchi	Life doubled, at least
Fatigue	AU4SG	Fin skin	Mirage	In service since 1978
Fatigue	AU4SG	Lower wing skin ^{ab}	Mirage	Over 150 repairs since 1979
Fatigue	2024T3	Upper wing skin	Nomad (fatigue test)	Over 105 900 simulated flying hours
Fatigue	2024T3	Door frame	Nomad (fatigue test)	Over 106 619 simulated flying hours
Stress-corrosion	7075T6	Console truss	F111	Service since 1980
Lightning burn	2024T3	Fuselage skin	Orion	Service since 1980 ^c

Introduction: Why CFRP Laminates?

Traditional Strengthening Solutions:

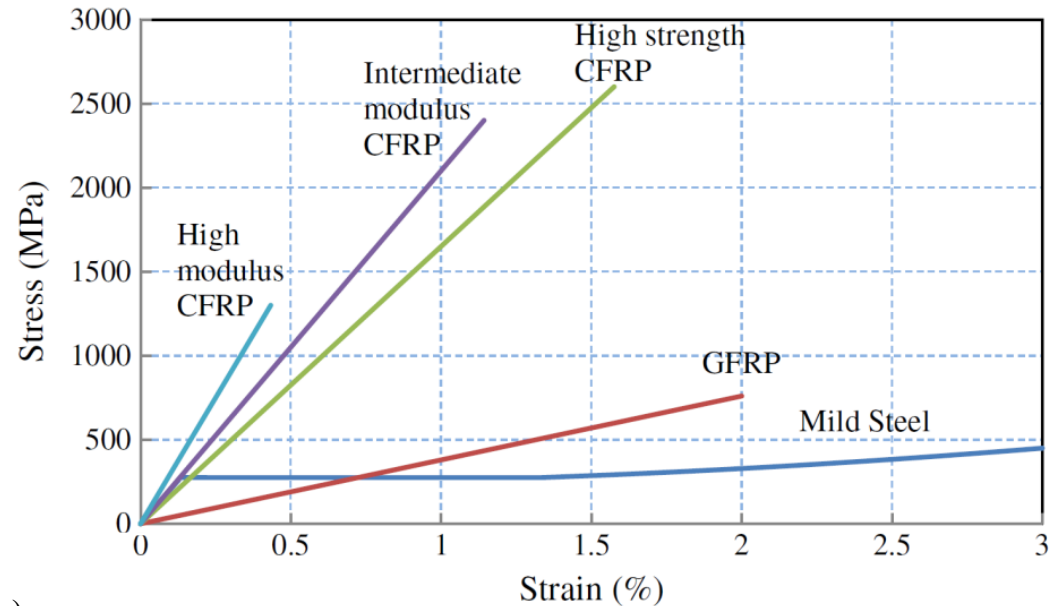
- Steel: heavy

CFRP:

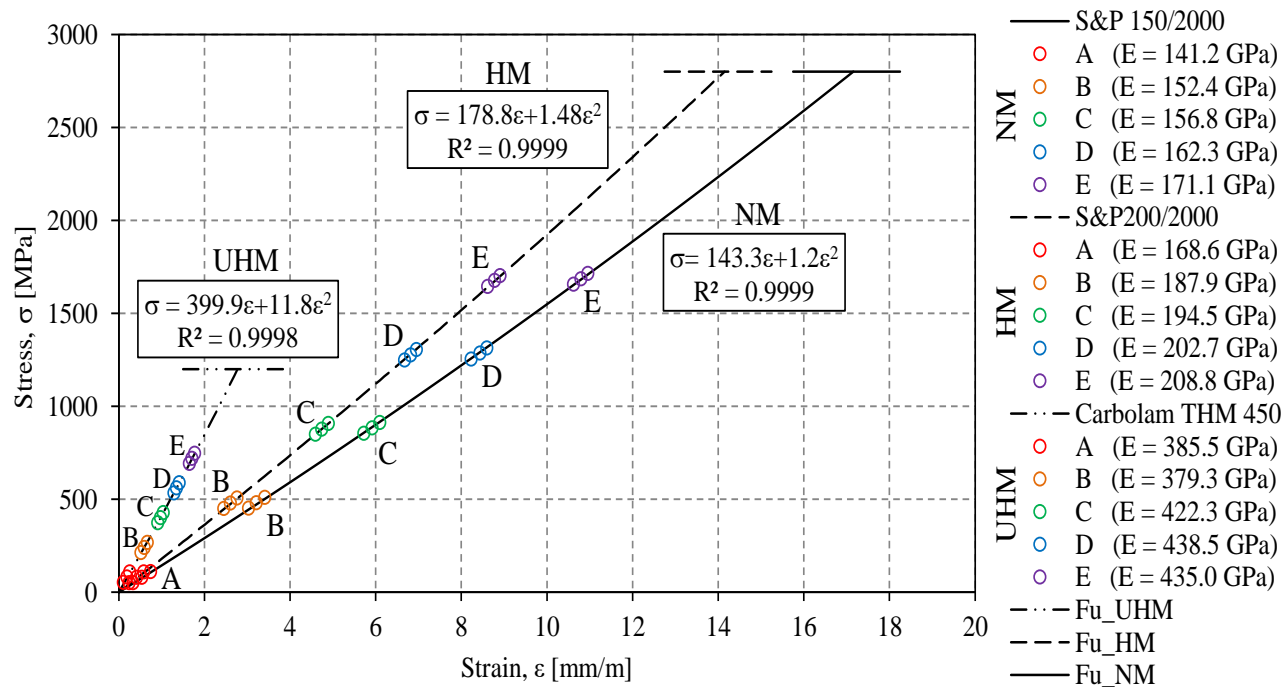
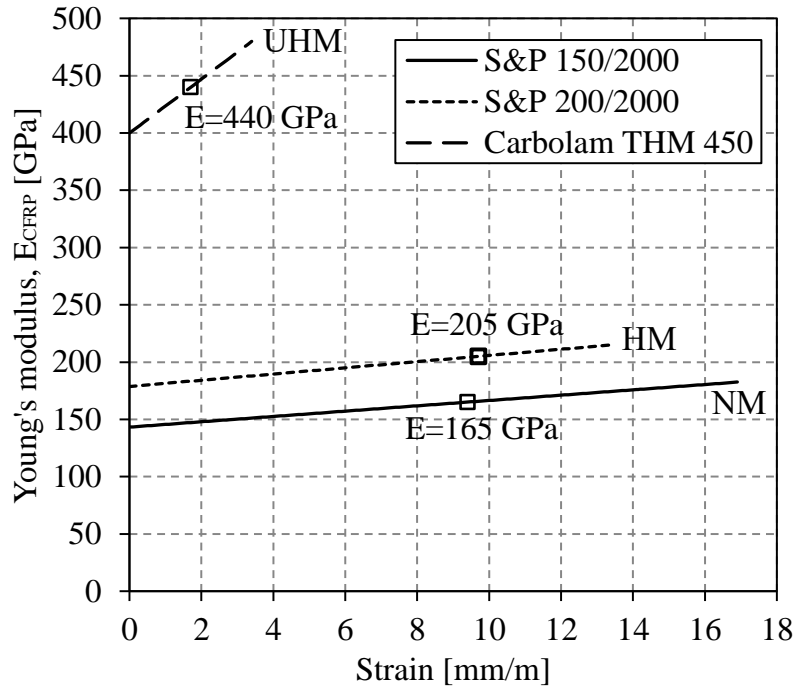
- Excellent fatigue behavior
- High fatigue-to-weight ratio

Classifications of the CFRP laminates according to their Young's modulus relative to that of steel:

Laminate type	Laminate modulus
Low modulus (LM)	$< 100 \text{ GPa}$ ($E_{\text{CFRP}} < 0.5 E_{\text{steel}}$)
Normal modulus (NM)	$100 - 200 \text{ GPa}$ ($0.5 E_{\text{steel}} \leq E_{\text{CFRP}} < E_{\text{steel}}$)
High modulus (HM)	$200 - 400 \text{ GPa}$ ($E_{\text{steel}} \leq E_{\text{CFRP}} < 2 E_{\text{steel}}$)
Ultra-high modulus (UHM)	$\geq 400 \text{ GPa}$ ($E_{\text{CFRP}} \geq 2 E_{\text{steel}}$)



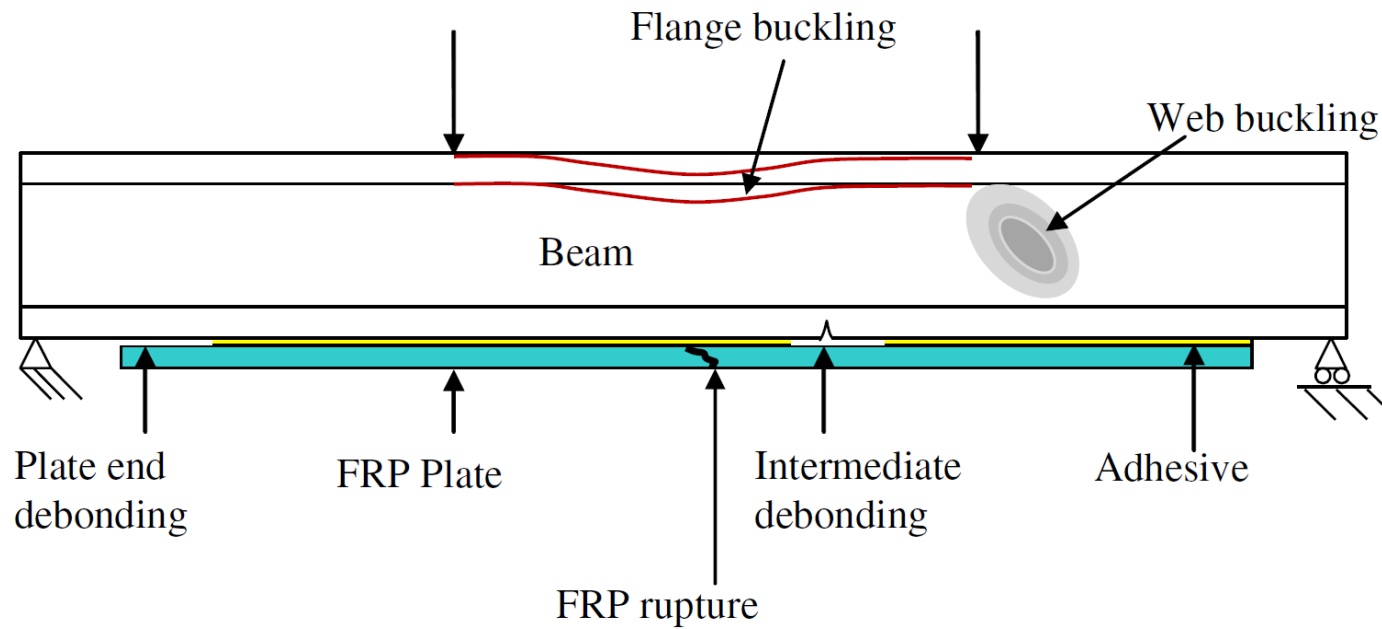
Introduction: Change in CFRP Young's Modulus



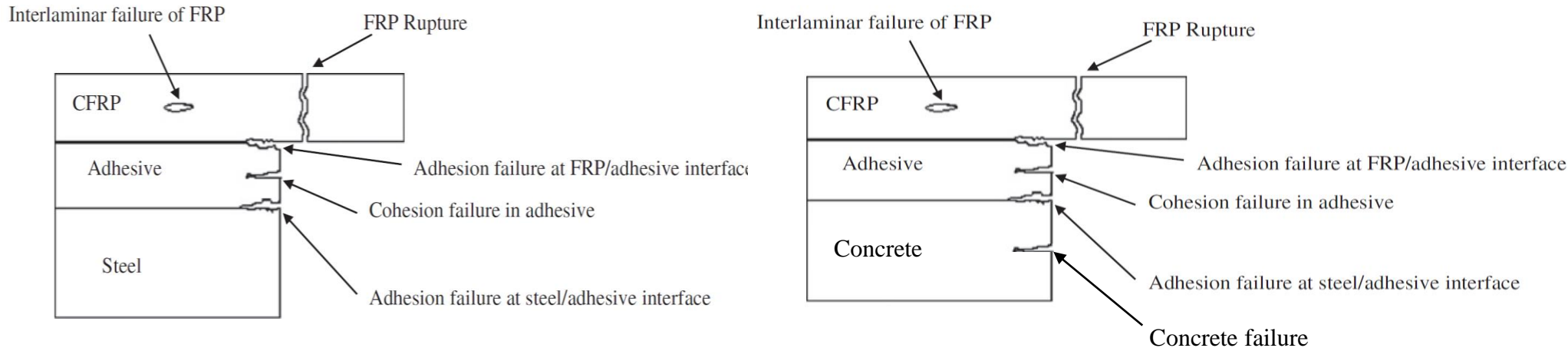
The measured Young's modulus of the NM, HM, and UHM CFRP laminates as a function of the applied strain. The square markers show the Young's moduli provided by the manufacturers.

The measured Young's modulus for the NM, HM, and UHM CFRP laminates at different strain levels, indicating a non-linear elastic behavior for the CFRP laminates.

Introduction: Some of Typical Failure Modes of Steel Beams Bonded with CFRP Plate



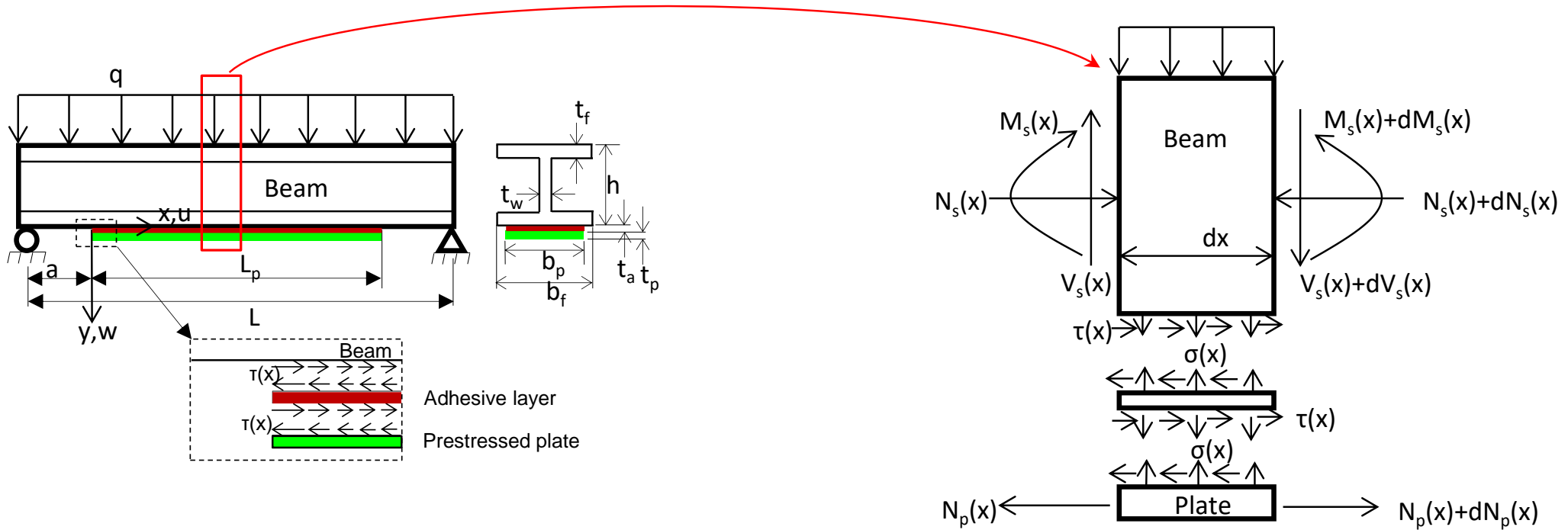
Introduction: Possible Failure Modes of CFRP-to-Concrete/Steel Bonded Joints

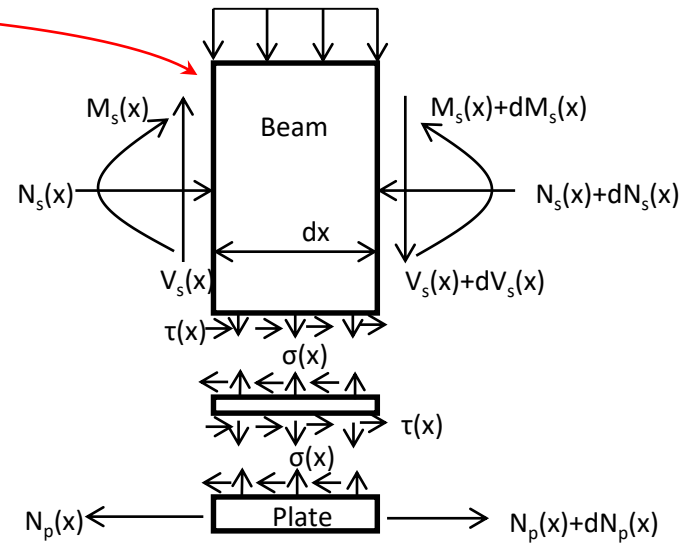
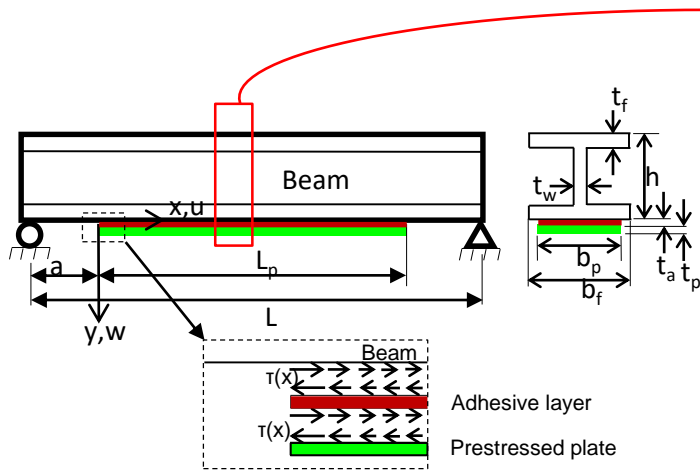


- The main difference between FRP–steel and FRP–concrete bonded joints is that in the former, failure will likely occur in the adhesive layer and in the latter failure is expected to occur in the concrete. Therefore, by providing an adequate bond length, the optimal strength of a bond joint is dependent on the fracture energy of the adhesive for the former and the fracture energy of the concrete for the latter.
- In FRP-strengthened steel structures, interfacial failure should happen within the adhesive layer in the form of **cohesion** failure to maximize the effectiveness of FRP strengthening.
- Inappropriate surface preparation of the steel substrate prior to the bond application may result in an adhesion failure at the steel-to-adhesive interface.

Flexural Strengthening

Steel Beam Strengthened by a Prestressed Bonded Plate





$$N_s(x) = N_p(x) = N(x) \quad (1)$$

$$\varepsilon_s(x) = \frac{du_s(x)}{dx} = \varepsilon_s^N(x) + \varepsilon_s^M(x) = -\frac{du_s^N(x)}{dx} + \frac{hM_s(x)}{2E_s I_s} \quad (2)$$

$$\varepsilon_p(x) = \frac{du_p(x)}{dx} = \frac{\Delta N_p(x)}{E_p A_p} \quad (3)$$

$$\Delta N_p(x) = N_p(x) - N_0 \quad (4)$$

$$\tau(x) = \frac{G_a}{t_a} (u_p(x) - u_s(x)) \quad (5)$$

$$\frac{d\tau(x)}{dx} = \frac{G_a}{t_a} \left(\frac{du_p(x)}{dx} - \frac{du_s(x)}{dx} \right) \quad (6)$$

$$(2) \ \& \ (3) \ \text{into} \ (6) \Rightarrow \frac{d\tau(x)}{dx} = \frac{G_a}{t_a} \left(\frac{N_p(x) - N_0}{E_p A_p} - \frac{hM_s(x)}{2E_s I_s} + \frac{N_s(x)}{E_s A_s} \right) \quad (7)$$

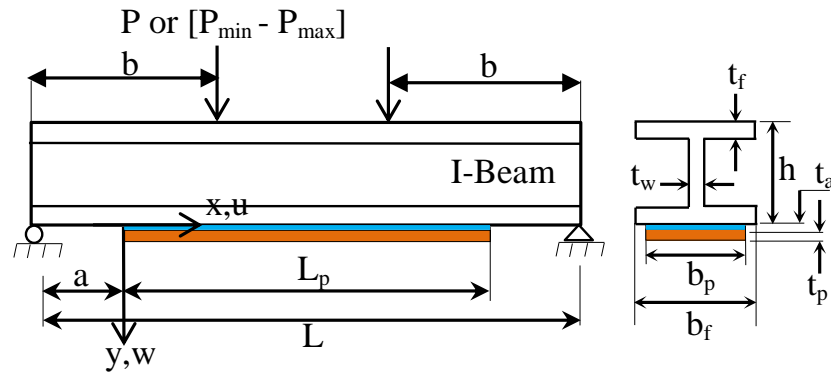
$$\frac{d^2\tau(x)}{dx^2} = \frac{G_a}{t_a} \left(\frac{1}{E_p A_p} \frac{dN_p(x)}{dx} - \frac{h}{2E_s I_s} \frac{dM_s(x)}{dx} + \frac{1}{E_s A_s} \frac{dN_s(x)}{dx} \right) \quad (8)$$

$$\text{Force equilibrium in x direction: } \frac{dN_s(x)}{dx} = \frac{dN_p(x)}{dx} = b_p \tau(x) \quad (9)$$

$$\text{Moment equilibrium: } \frac{dM_s(x)}{dx} = V_s(x) - \frac{b_p h}{2} \tau(x) \quad (10)$$

$$\frac{d^2\tau(x)}{dx^2} - \frac{G_a b_p}{t_a} \left(\frac{1}{E_s I_s} + \frac{1}{E_p I_p} + \frac{h^2}{4I_s E_s} \right) \tau(x) = -K \frac{h}{2E_s I_s} V_T(x) \quad (11)$$

$$\frac{d^2\tau(x)}{dx^2} - \alpha\tau(x) = \beta(x) \quad (12)$$



Beam strengthened by the bonded CFRP laminate in a four-point bending set-up.

By applying the boundary conditions for the above four-point bending set-up:

$$\tau(x) = \begin{cases} \left(\frac{G_a}{t_a \lambda} \left(\frac{N_0}{E_p A_p} + \frac{hPa}{2E_s I_s} \right) e^{-\lambda x} + m_1 P (1 - e^{-\lambda \mu} \cosh(\lambda x)) \right) & 0 \leq x \leq b - a \\ \left(\frac{G_a}{t_a \lambda} \left(\frac{N_0}{E_p A_p} + \frac{hPa}{2E_s I_s} \right) + m_1 P \sinh(\lambda \mu) \right) e^{-\lambda x} & b - a \leq x \leq L_p / 2 \end{cases} \quad (13)$$

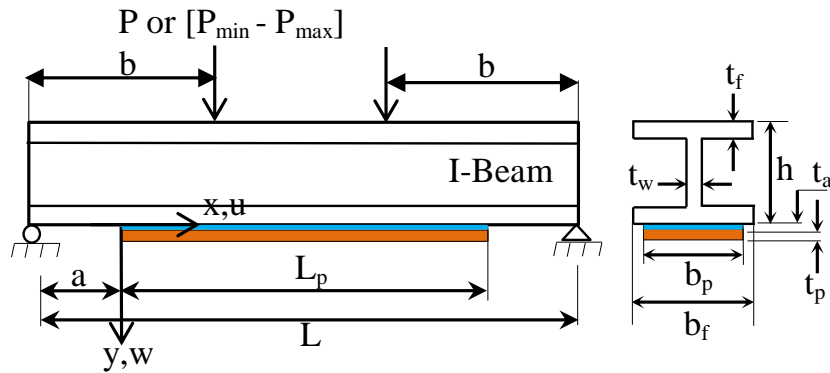
$$\lambda = \sqrt{\frac{G_a b_p}{t_a} \left(\frac{1}{E_s I_s} + \frac{1}{E_p I_p} + \frac{h^2}{4E_s I_s} \right)}; \quad m_1 = \frac{G_a}{2t_a \lambda^2} \frac{h}{E_s I_s} \quad (14)$$

$$\text{From (1) \& (7) } \Rightarrow N(x) = \frac{b_p}{\lambda^2} \left(\frac{d\tau(x)}{dx} + m_1 \lambda^2 M_T(x) + \frac{G_a N_0}{t_a E_p A_p} \right) \quad (15)$$

(16)

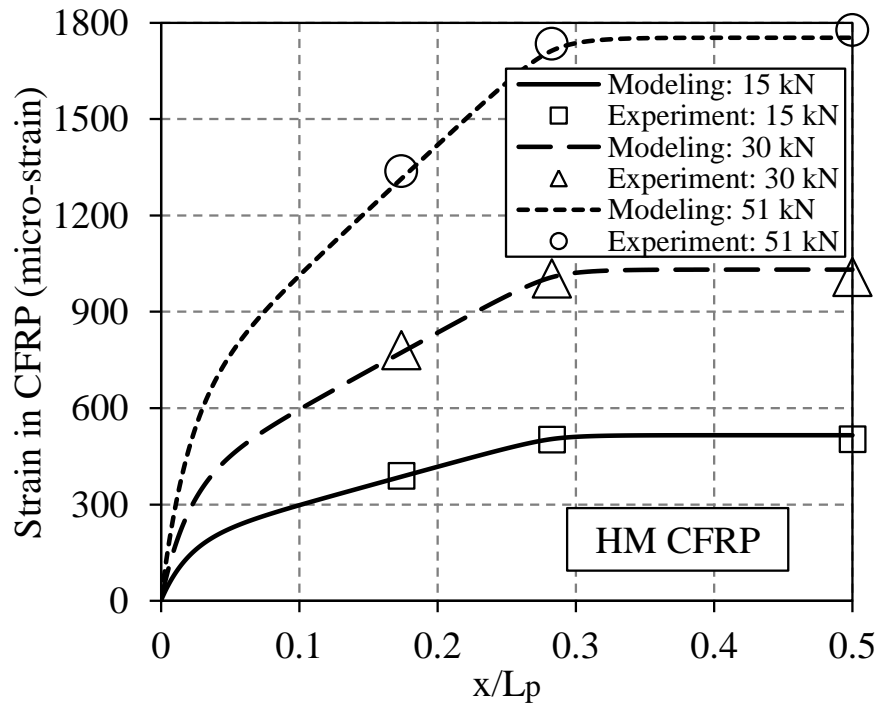
Stress in bottom flange:

$$\sigma(x) = M_T(x) \frac{h}{2I_s} - \frac{b_p}{\lambda^2} \left(\frac{h^2}{4I_s} + \frac{1}{A_s} \right) \left(\frac{d\tau(x)}{dx} + m_1 \lambda^2 M_T(x) + \frac{G_a N_0}{t_a E_p A_p} \right) \quad (17)$$

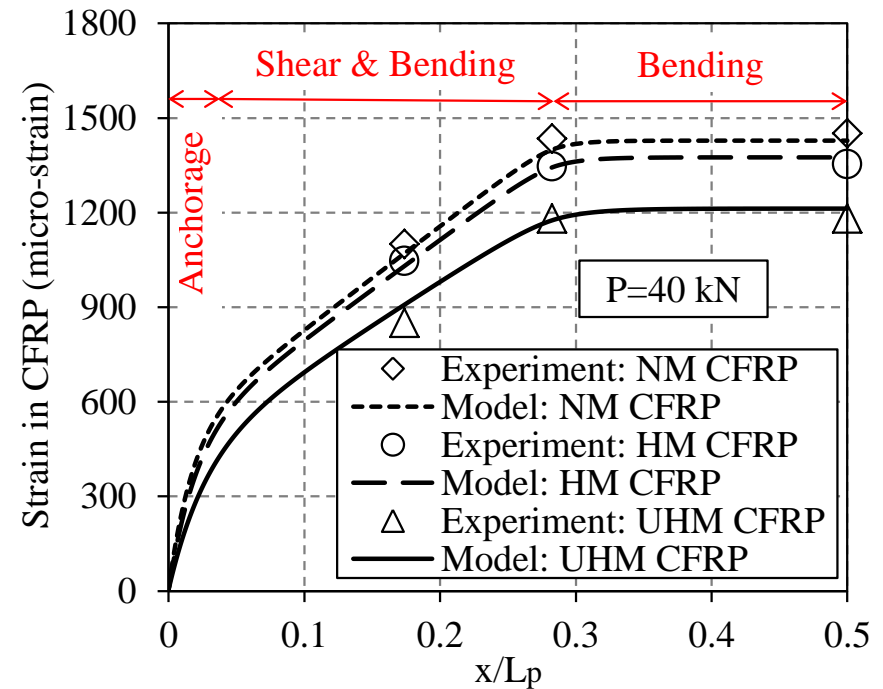


A simply supported beam with a free span of $L=1200$ mm and a CFRP plate length of $L_p=920$ mm (i.e., $a=140$ mm) in a four-point bending set-up:

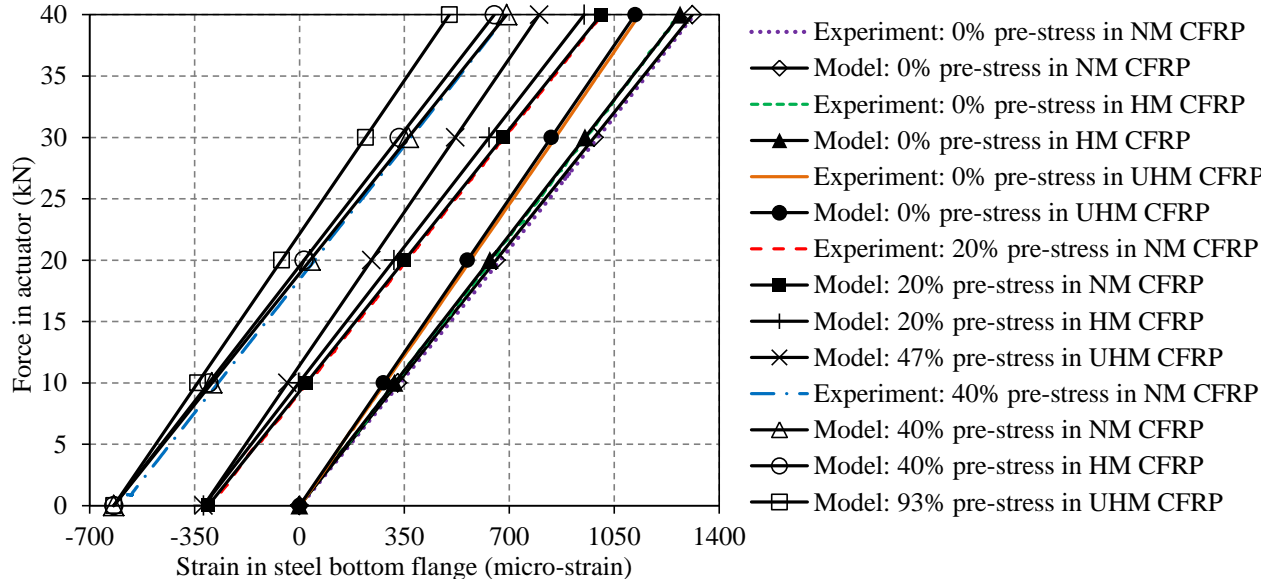
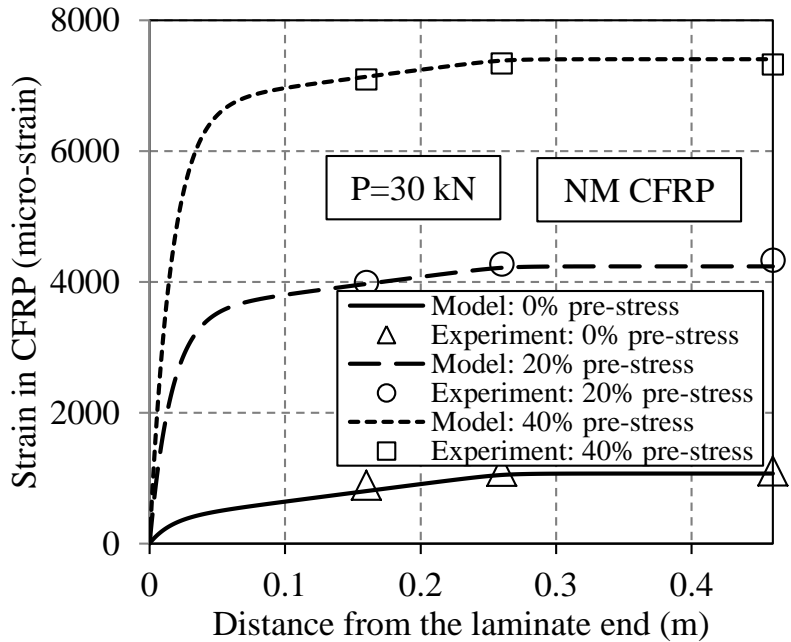
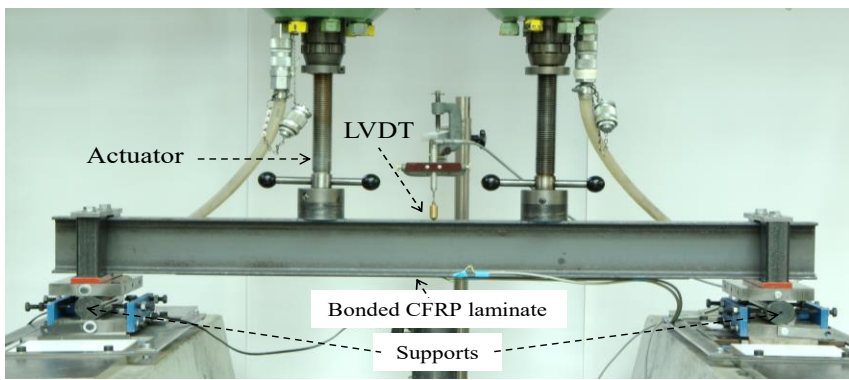
$b_f = 65$ mm, $t_f = 6.2$ mm, $t_w = 4.4$ mm, $h = 120$ mm, $t_p = 1.4$ mm, $b_p = 50$ mm, $t_a = 1$ mm, $E_s = 210$ GPa, $G_a = 1040$ MPa.



The calculated and measured strains along the CFRP laminates for the beam strengthened by the HM CFRP at actuator load levels of $P=15$ kN, 30 kN and 51 kN (within the elastic domain).

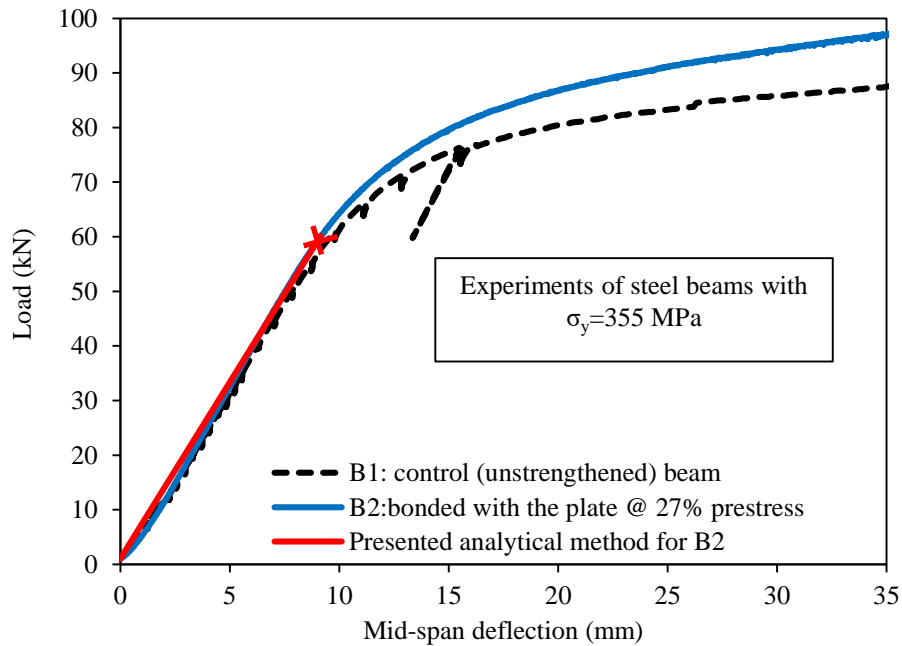
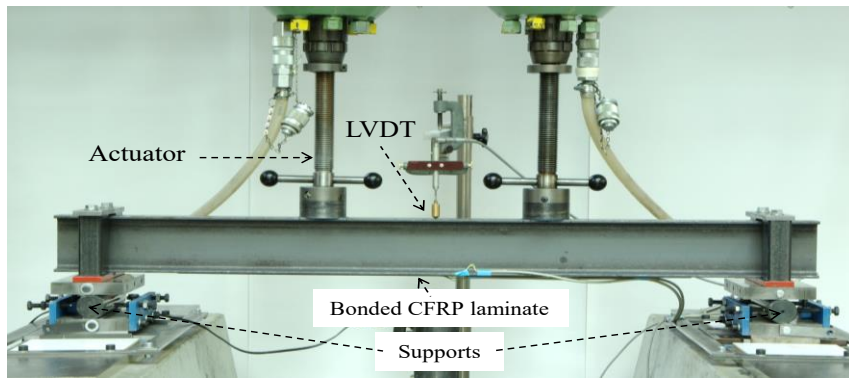


The calculated and measured strain along the CFRP laminates for the retrofitted beams with the NM, the HM and the UHM CFRP at an actuator load level of $P=40$ kN (within the elastic domain).

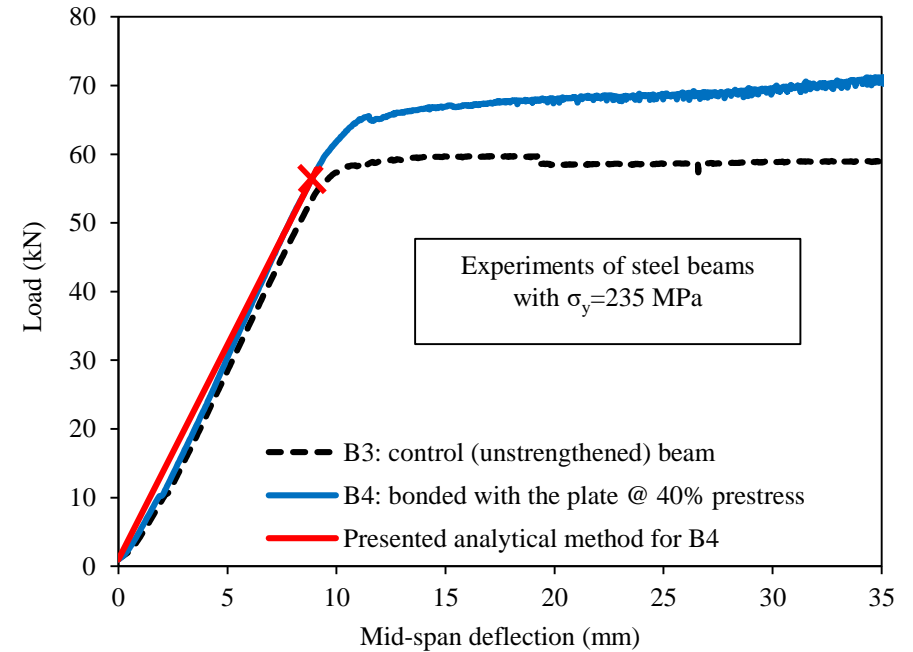


The calculated and measured strains along the CFRP laminates for the beams strengthened by the NM CFRP with 0%, 20% and 40% pre-stress levels subjected to an actuator load level of P=30 kN.

The strain in the bottom flange of the specimens strengthened by the NM, the HM and the UHM CFRP laminates with different pre-stress levels while the actuator load, P, increases from 0 to 40 kN.



Comparison of load-deflection behaviors of steel beams with $\sigma_y=355\text{ MPa}$, one unstrengthened and one strengthened with a 27% prestressed bonded CFRP plate, both loaded in a four-point bending set-up.

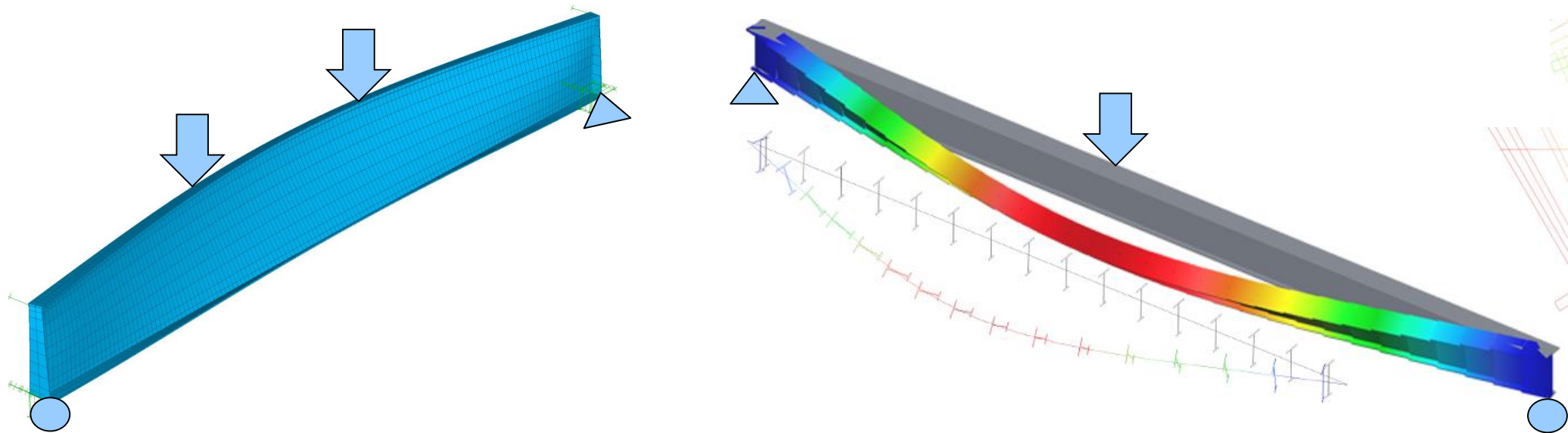


Comparison of load-deflection behaviors of two steel beams with $\sigma_y=235\text{ MPa}$, one unstrengthened and one strengthened with a 40% prestressed bonded CFRP plate, both loaded in a four-point bending set-up

Strengthening against Lateral Torsional Buckling

Definition of Lateral Torsional Buckling (LTB)

- The LTB failure is often triggered in slender beams, which do not have sufficient lateral supports, due to eccentricities, and can occur at load levels that are below yield capacity.
- These eccentricities, in reality, can be due to the geometrical imperfections of the beam itself or the position of the loads.
- The eccentricity generates a bending moment about the longitudinal axis, which displaces the compression flange laterally away from the loading plane, while the tension flange tends to keep the beam straight, and thus, the beam cross section is twisted.
- This twisting in combination with the lateral displacement of the beam is called the LTB failure and could occur well before the yielding capacity of the steel cross section is reached.



Mechanisms of Strengthening against LTB

Two retrofit mechanisms:

- Increasing out-of-plane stiffness of the beam using **UHM CFRP laminates**

For the LTB failure, the specimen buckles out of the plane under flexural loading, and the CFRP laminates can affect the buckling capacity of the retrofitted beams by stiffening the steel cross section around the weak axis. Application of the ultra-high modulus CFRP laminates increases the out-of-plane stiffness of the specimens, and consequently, the buckling strength of the beams increases.

- Applying tension to the top flange of the beam using **pre-stressed CFRP laminates**

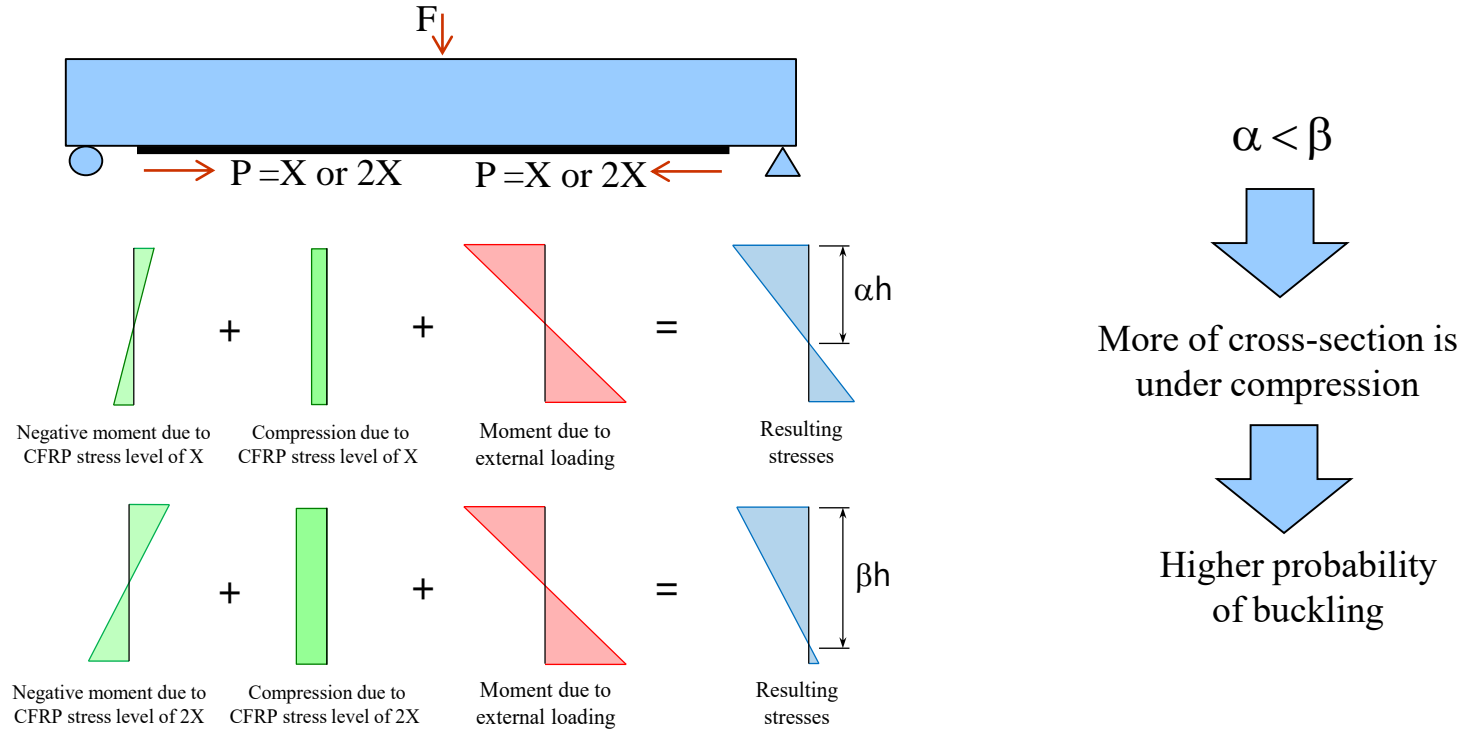
Whether the prestressed CFRP laminate leads to tensile or compressive stresses in the top flange depends only on the profile geometry. Assuming that the prestressing is applied on the bottom surface of the bottom flange, the stresses in the top flange caused by the axial force and by the bending moment can be calculated as:



$$\sigma_{\text{top}} = \frac{ph/2}{I} \times \frac{h}{2} - \frac{P}{A} > 0 \Rightarrow h > 2 \cdot \sqrt{\frac{I}{A}} \quad \text{Condition for top flange to be in tension}$$

Important Notes on CFRP Strengthening against LTB

- When $h < 2 \cdot \sqrt{\frac{I}{A}}$, use of CFRP laminates with high pre-stress levels is NOT recommended! Instead, we can use UHM laminates.



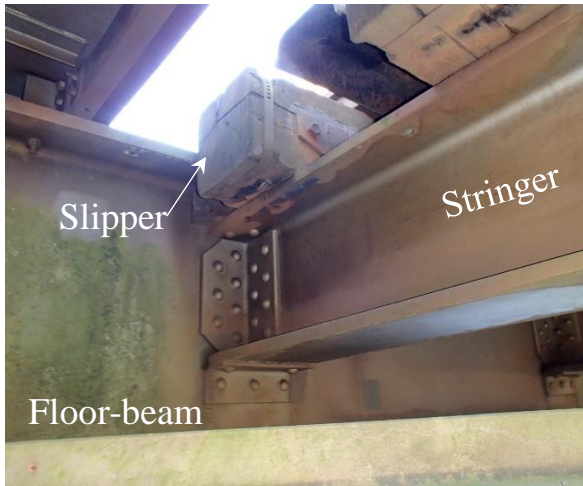
Stress distribution in the beam cross-section for the two different pre-stress levels of $X\%$ and $2X\%$.

- Note: Application of CFRP laminates to the tension face of the steel beams increases the in-plane bending strength and also the lateral buckling strength; however, the former increases more significantly. This arrangement could change the failure mode of the steel beam from in-plane bending to the buckling failure mode after CFRP strengthening. This need to be check in advance!

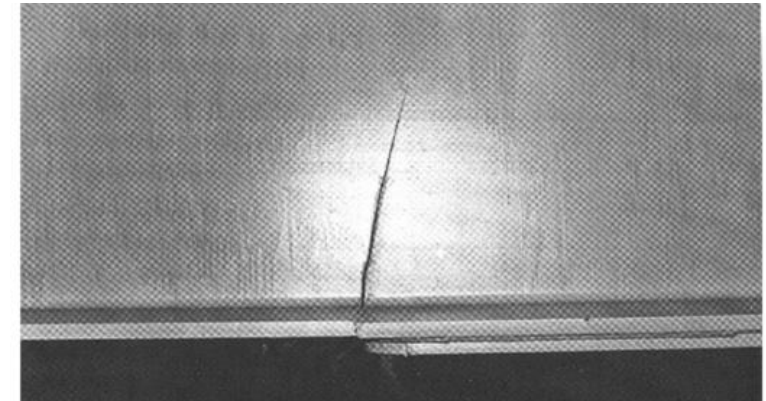
Fatigue Strengthening

Fatigue Strengthening

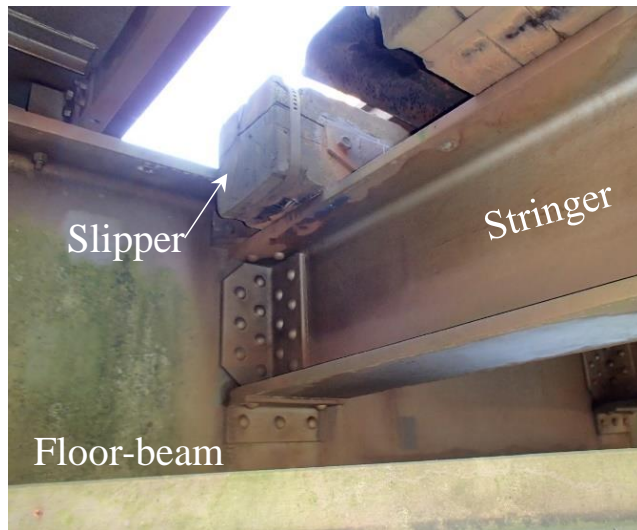
- Healthy metallic members:



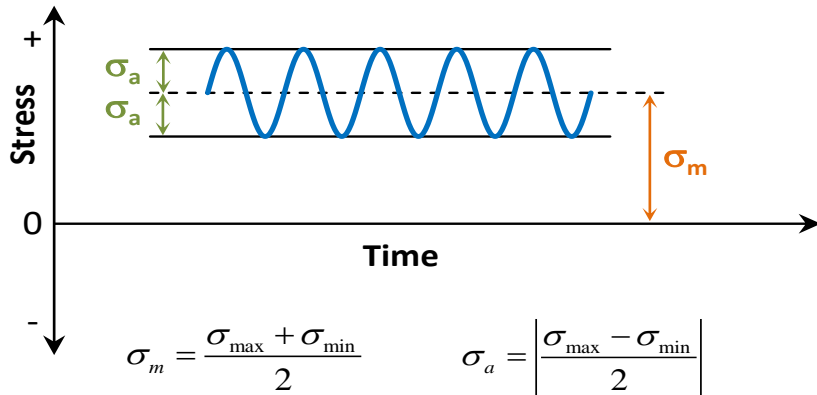
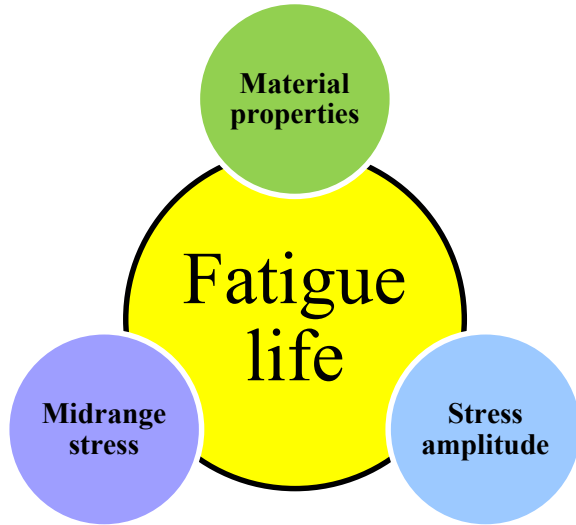
- Cracked metallic members:



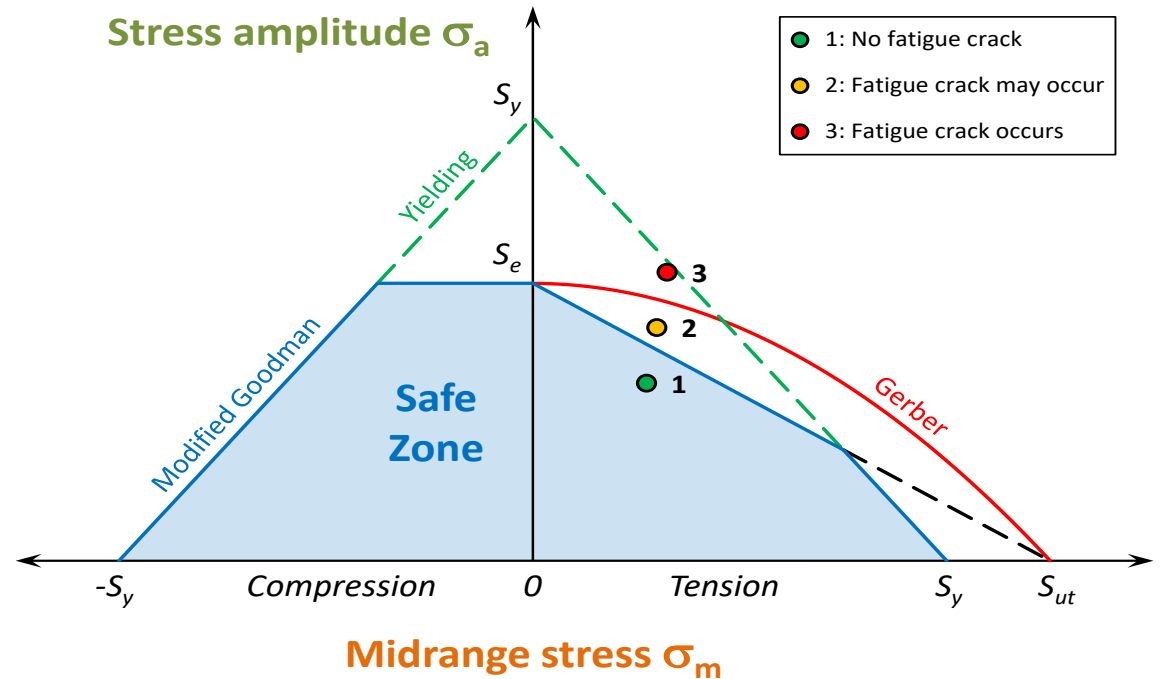
Fatigue Strengthening of Healthy Metallic Members



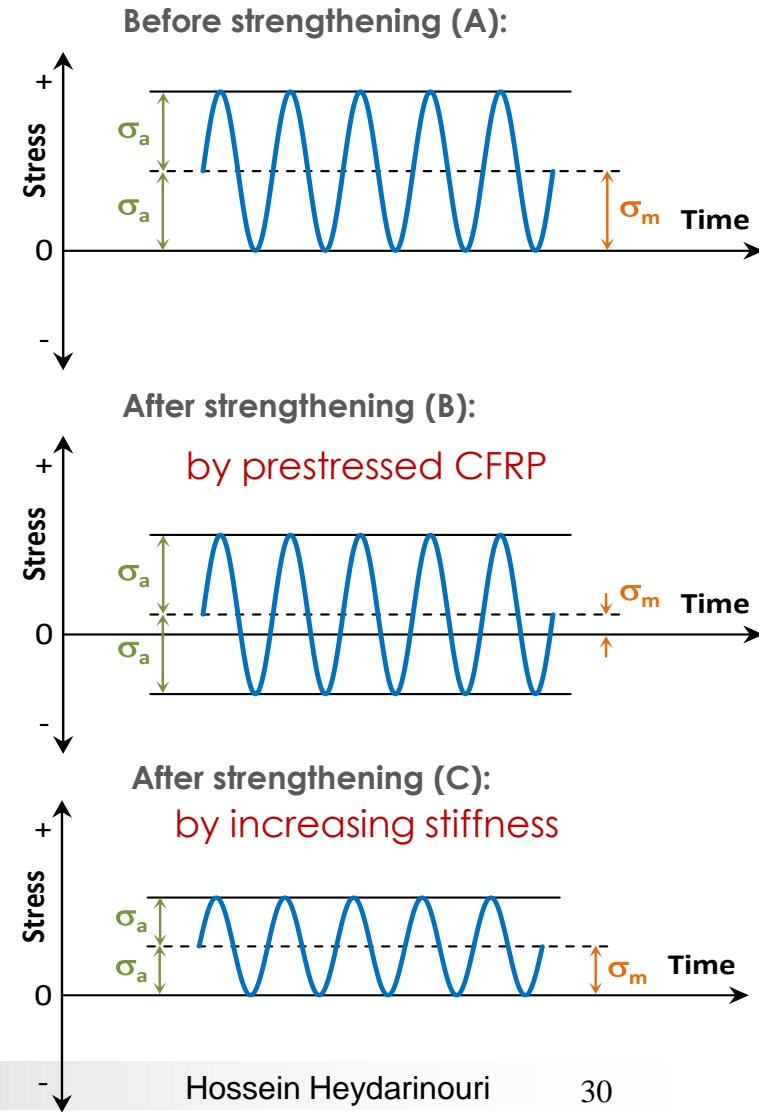
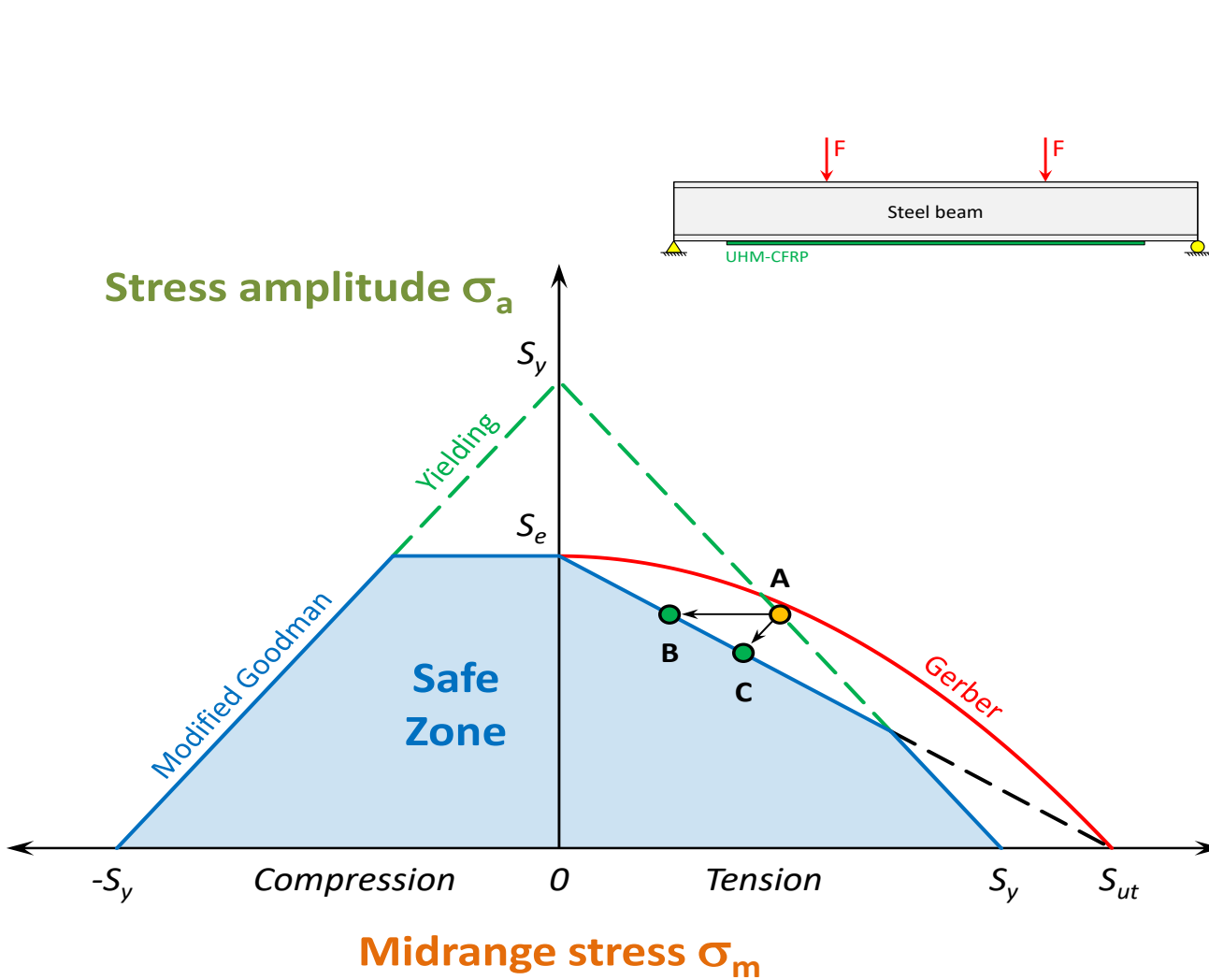
Fatigue Theory



S_y Yield strength
 S_e Fatigue endurance limit
 S_{ut} Ultimate tensile strength



Fatigue Theory



Fatigue Theory

$$\frac{d^2\tau(x)}{dx^2} - \frac{G_a b_p}{t_a} \left(\frac{1}{E_s I_s} + \frac{1}{E_p I_p} + \frac{h^2}{4E_s I_s} \right) \tau(x) = -\frac{G_a}{t_a} \frac{h}{2E_s I_s} V_T(x)$$

$$\tau(x) = \left(\frac{G_a}{t_a \lambda} \left(\frac{N_0}{E_p A_p} + \frac{hPa}{2E_s I_s} \right) + m_1 P \sinh(\lambda \mu) \right) e^{-\lambda x}$$

$$\sigma_{flange} = \frac{hPa}{2I_s} - b_p \left(\frac{h^2}{4I_s} + \frac{1}{A_s} \right) \left(-\frac{\tau(L_p/2)}{\lambda} + m_1 Pa + \frac{G_a N_0}{\lambda^2 t_a E_p A_p} \right)$$

$\tau(x)$ interfacial shear stress along the CFRP plate

σ_{flange} stress in beam bottom flange

N force in CFRP plate

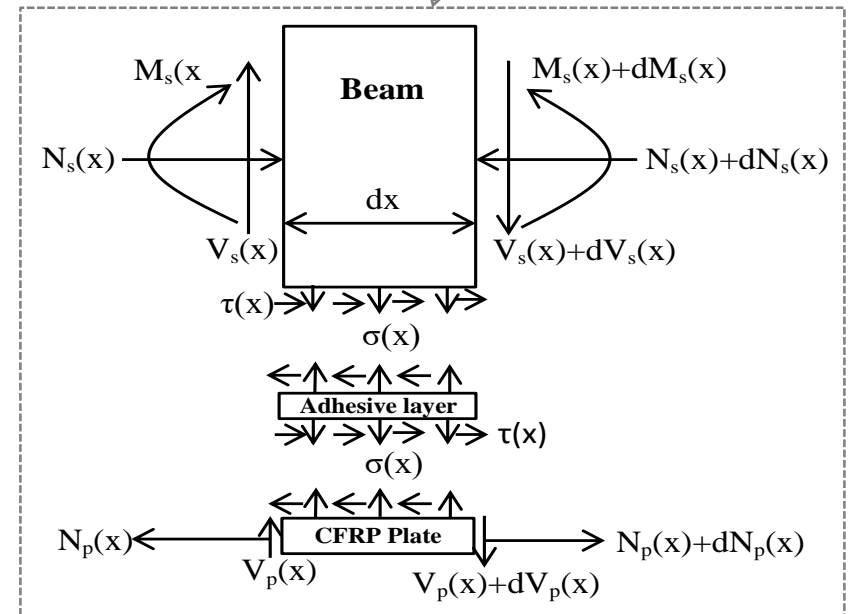
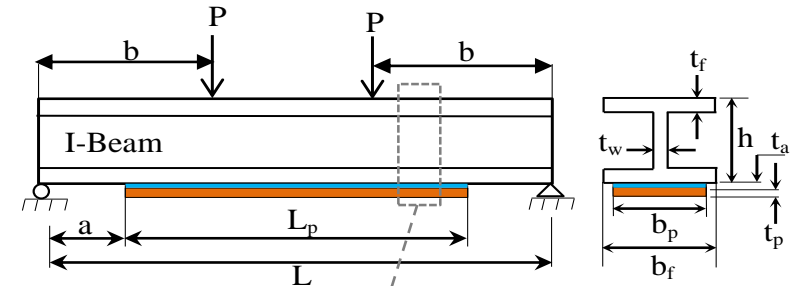
N_0 the pre-stress level

G_a adhesive shear modulus

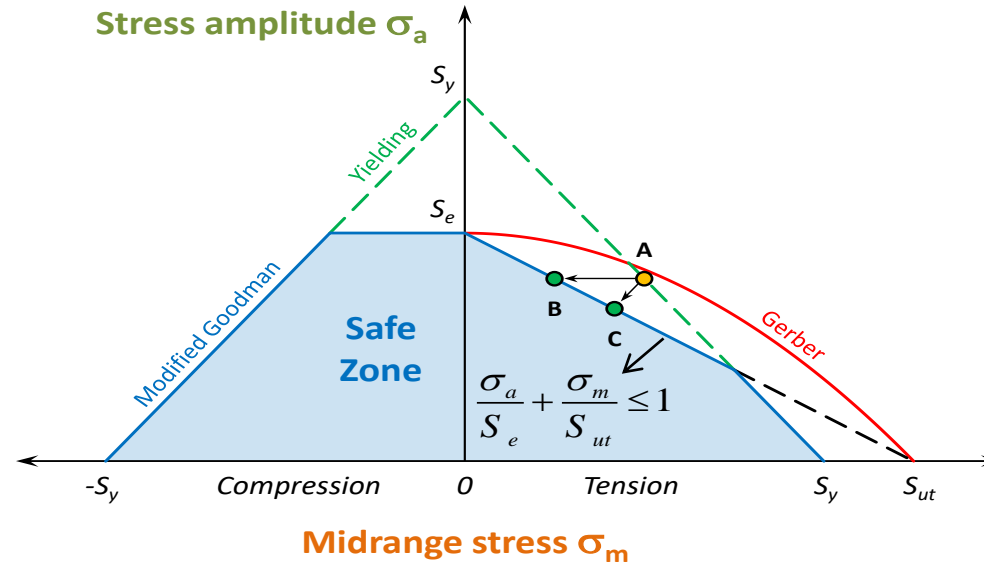
Note: Subscripts 's' and 'p' refers to the steel and the CFRP plate

$$\lambda = \sqrt{\frac{G_a b_p}{t_a} \left(\frac{1}{E_s A_s} + \frac{1}{E_p A_p} + \frac{h^2}{4E_s I_s} \right)}$$

$$m_1 = \frac{G_a}{2t_a \lambda^2} \frac{h}{E_s I_s}$$



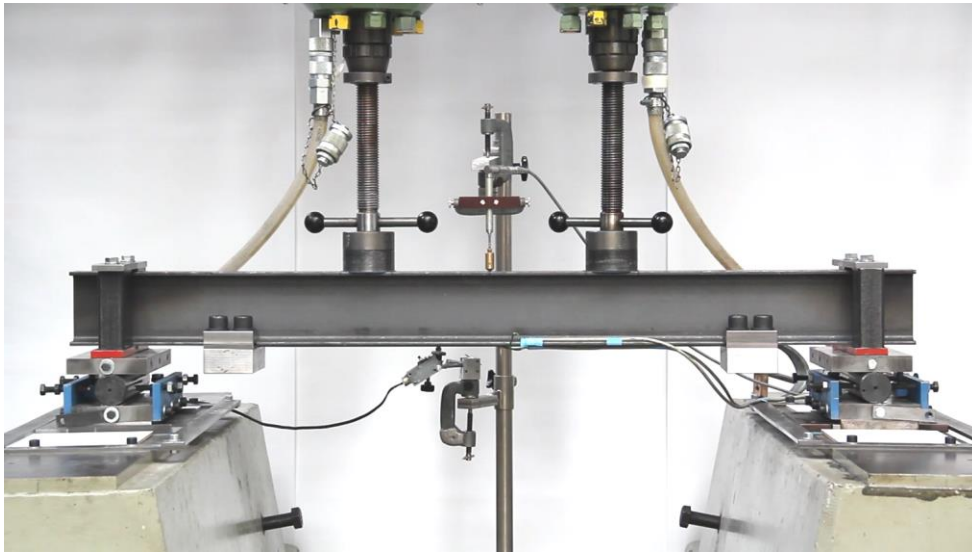
Fatigue Theory



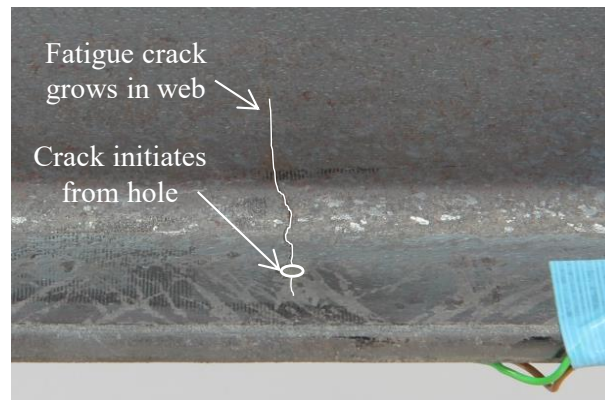
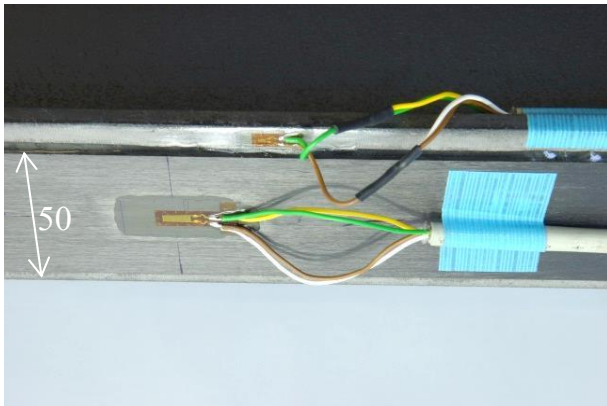
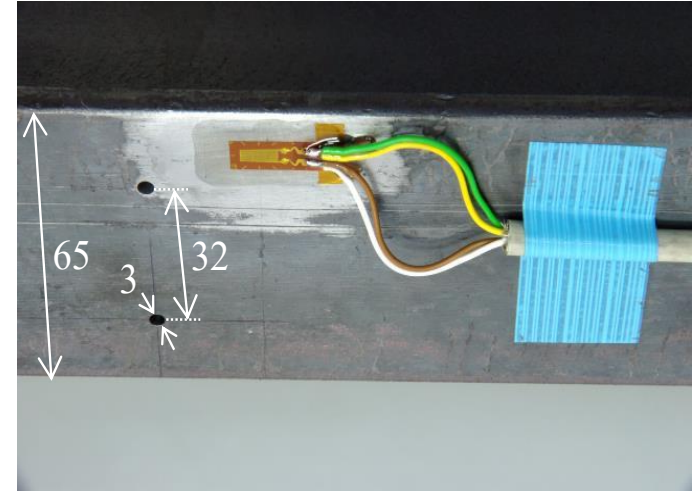
$$\sigma_{flange} = \frac{hPa}{2I_s} - b_p \left(\frac{h^2}{4I_s} + \frac{1}{A_s} \right) \left(-\frac{\tau(L_p/2)}{\lambda} + m_1 Pa + \frac{G_a N_0}{\lambda^2 t_a E_p A_p} \right)$$

$$\frac{haP_a}{2I_s S_e} - \frac{b_p}{S_e} \left(\frac{h^2}{4I_s} + \frac{1}{A_s} \right) \left(m_1 a P_a + \frac{G_a N_0}{\lambda^2 t_a E_p A_p} \right) + \frac{haP_m}{2I_s S_{ut}} - \frac{b_p}{S_{ut}} \left(\frac{h^2}{4I_s} + \frac{1}{A_s} \right) \left(m_1 a P_m + \frac{G_a N_0}{\lambda^2 t_a E_p A_p} e^{-\lambda L_p/2} \right) \leq \frac{b_p - d}{nb_p k_f}$$

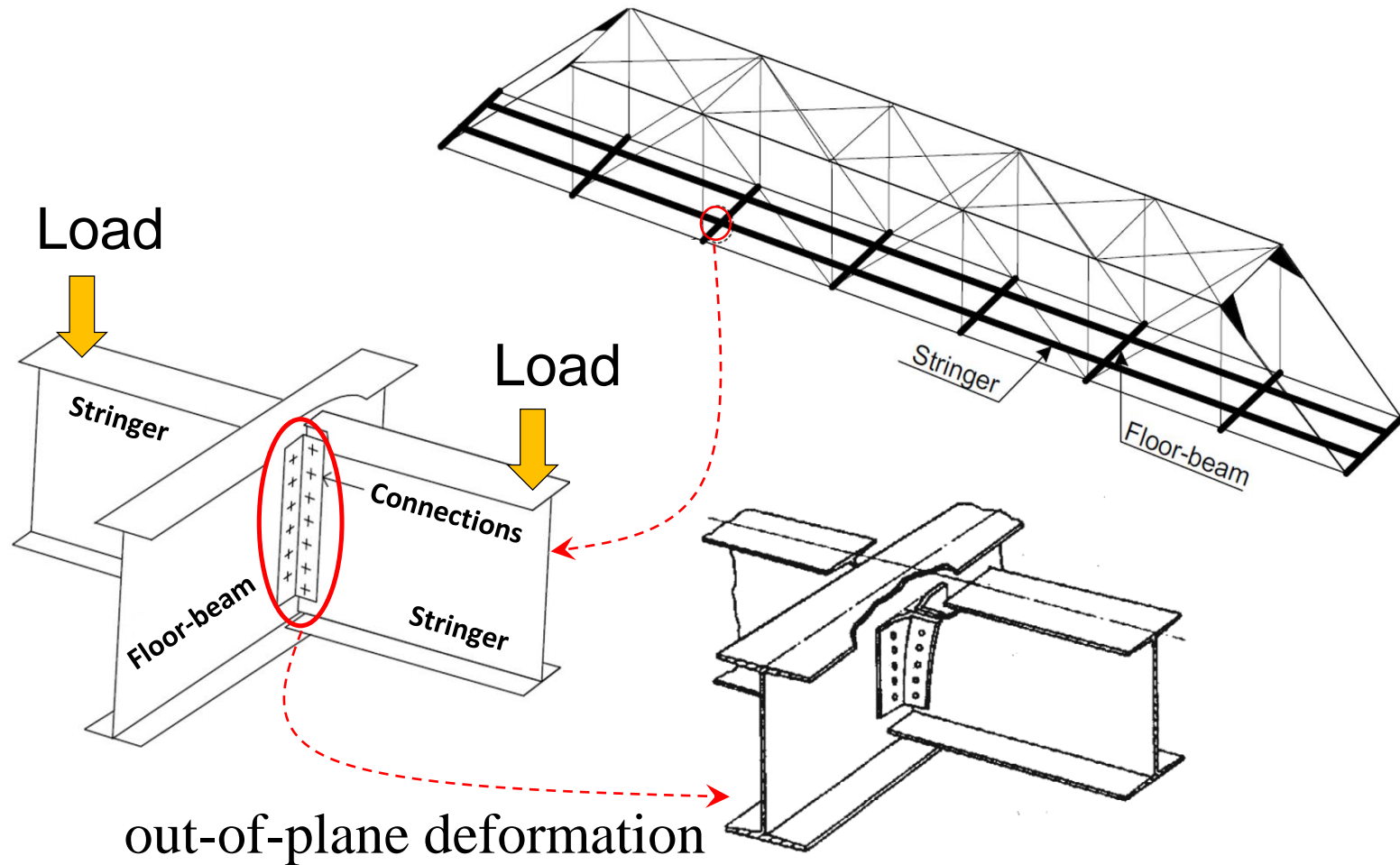
Laboratory Verifications



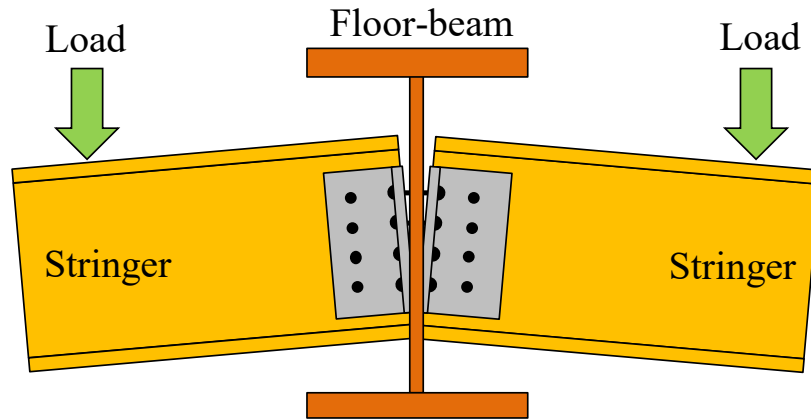
Video



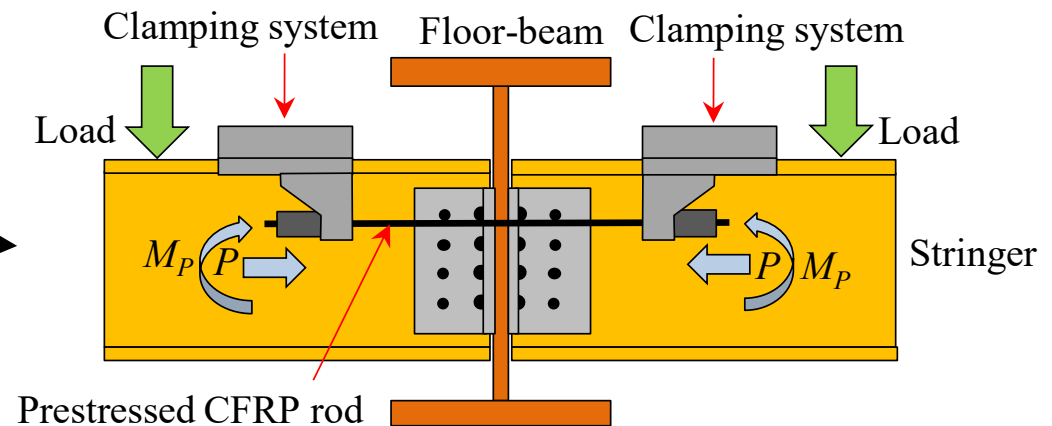
More complicated case: multiaxial fatigue



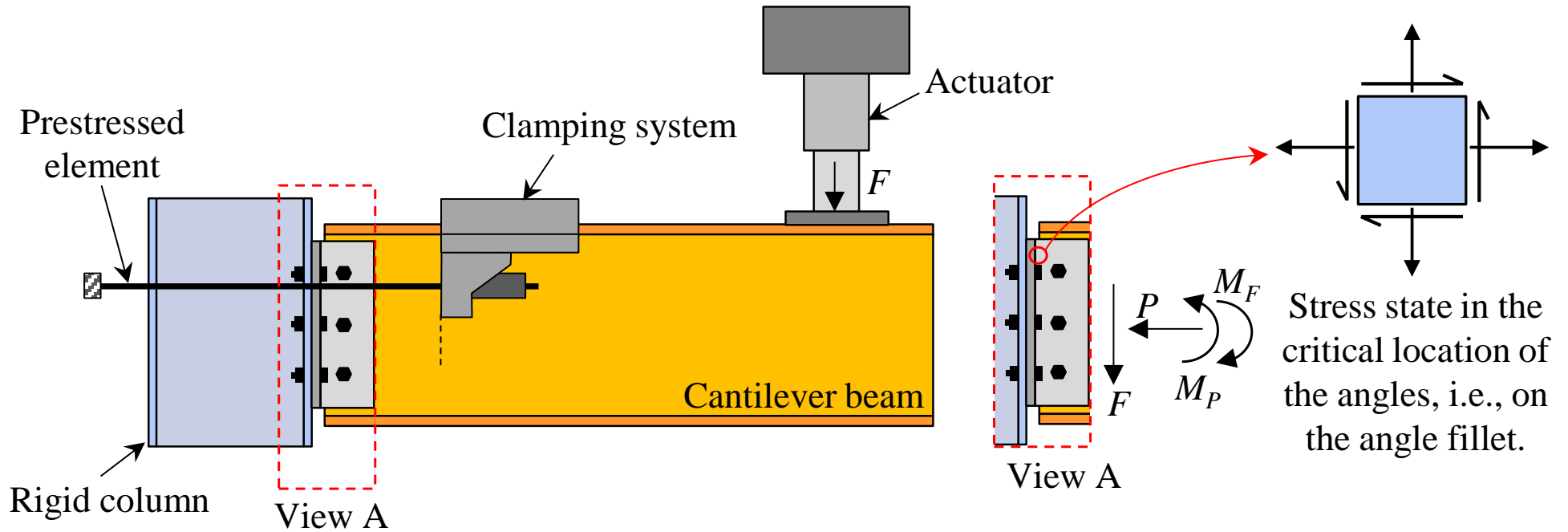
More complicated case: multiaxial fatigue



Reducing the out-of-plane deformation by prestressing force



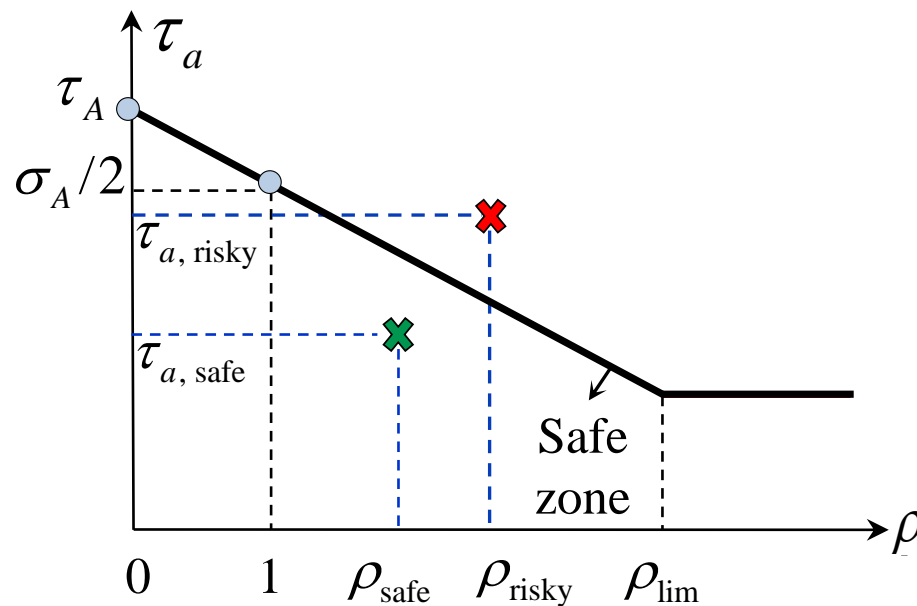
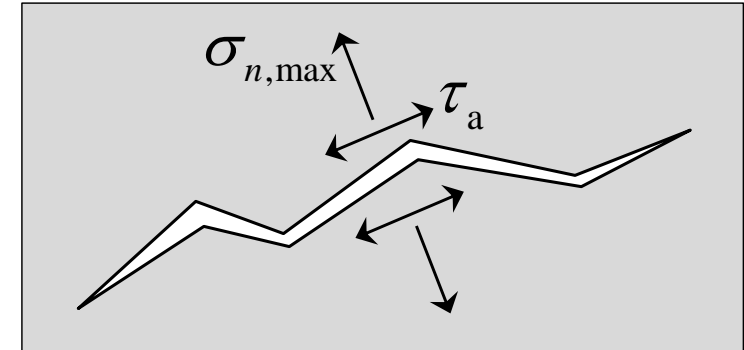
More complicated case: multiaxial fatigue



More complicated case: multiaxial fatigue

Critical plane approach

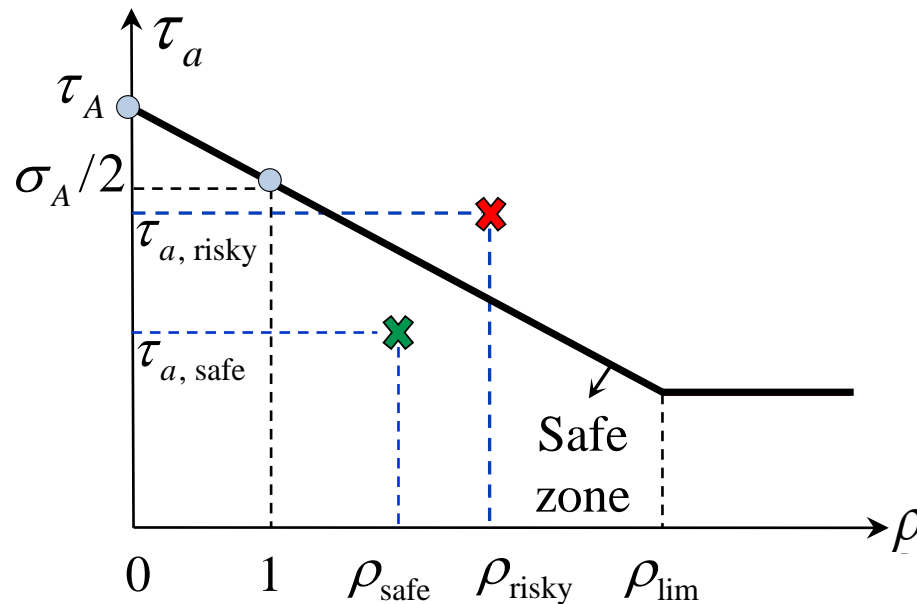
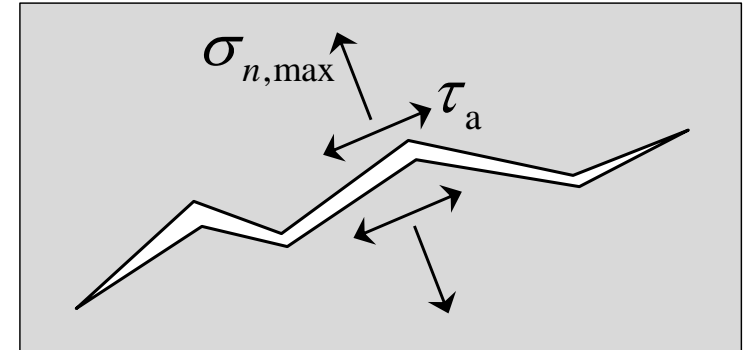
- τ_a : Maximum shear stress amplitude
- $\sigma_{n,\max}$: Maximum normal stress on the critical plane



More complicated case: multiaxial fatigue

Critical plane approach

- τ_a : Maximum shear stress amplitude
- $\sigma_{n,\max}$: Maximum normal stress on the critical plane



Conclusiones

➤ **The advantages of the proposed design approach:**

1. It is a proactive strengthening approach,
2. It takes into account the combined effects of mean stress and alternating stress levels.
3. It can be applied in more complicated case of multiaxial fatigue.

➤ **Two main fatigue retrofit mechanisms for healthy metallic members:**

1. to decrease the mean stress level by using pre-stressed laminate
2. to decrease mean and alternating stresses proportionally by using ultra-high modulus laminate

Case Study:
Fatigue Strengthening of Münchenstein Railway Bridge

Bridge History

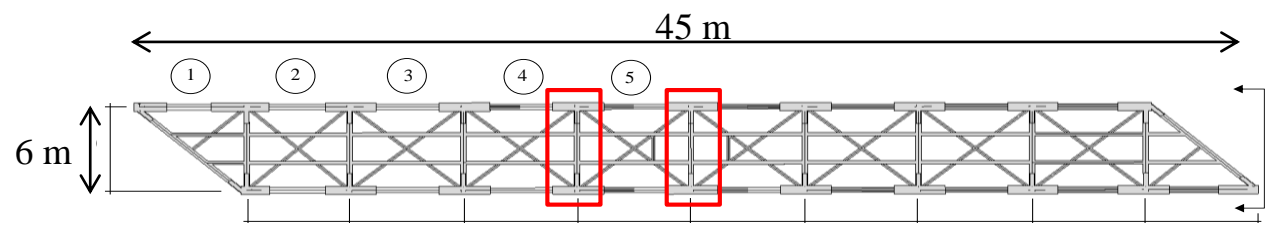
- The Münchenstein rail disaster on 1891 is historically the worst railway accident ever in Switzerland. The bridge had been built in 1875 by Gustave Eiffel, who built the Eiffel Tower later in 1889.
- Prof. Ludwig von Tetmajer, the first director of Empa, was commissioned to investigate the cause of this collapse. His investigation led to modification of Euler's formula for buckling of slender bars.



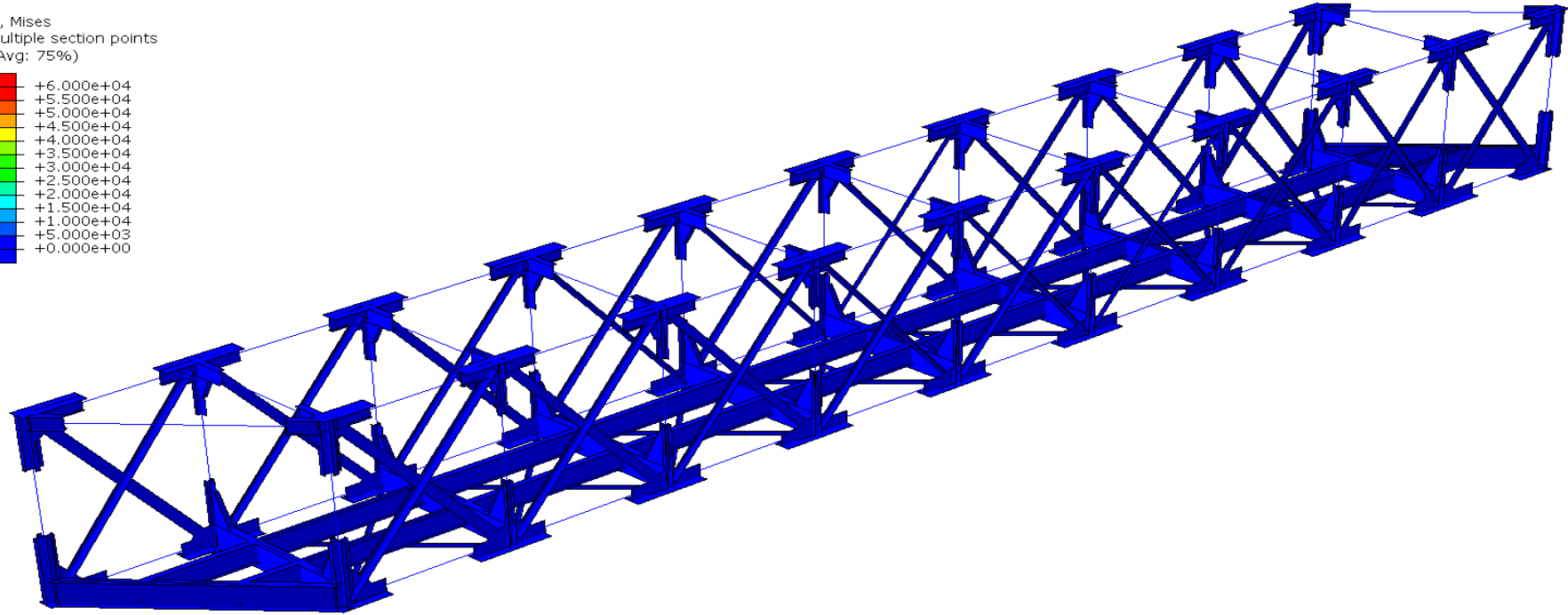
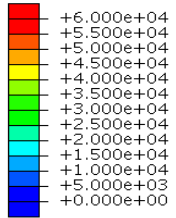
Bridge History

- Based on the verifications done by an engineering office*, the cross-beams of Münchenstein Bridge were the fatigue critical elements if further bridge serviceability after 2030 is intended.
- Therefore, the goal of a pilot project was to demonstrate the capability and the effectiveness of a pre-stressed un-bonded strengthening system to reinforce this bridge.

FE Modeling



S, Mises
Multiple section points
(Avg: 75%)



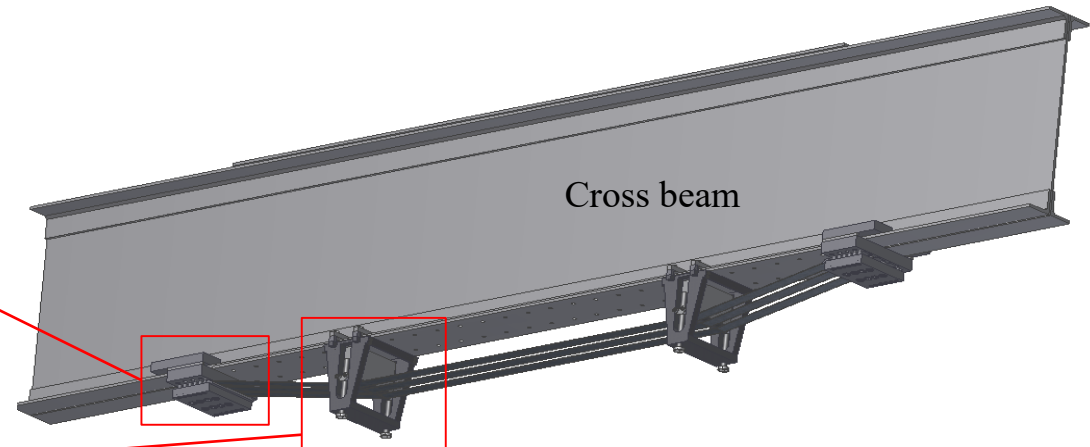
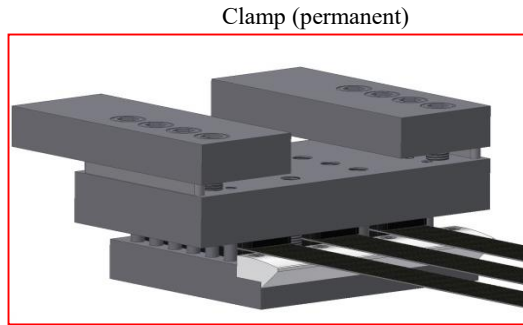
Step: Step-1
Increment 0: Step Time = 0.000
Primary Var: S, Mises
Deformed Var: U Deformation Scale Factor: +1.000e+02

Video

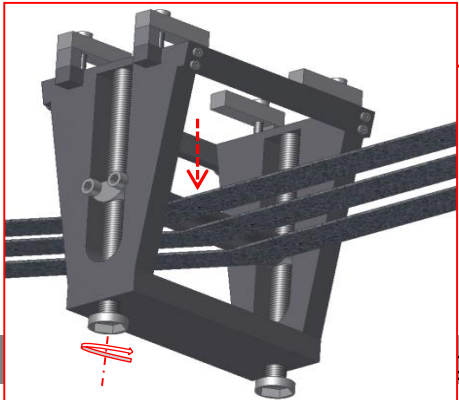
PUR System

Prestressed un-bonded retrofit (PUR)

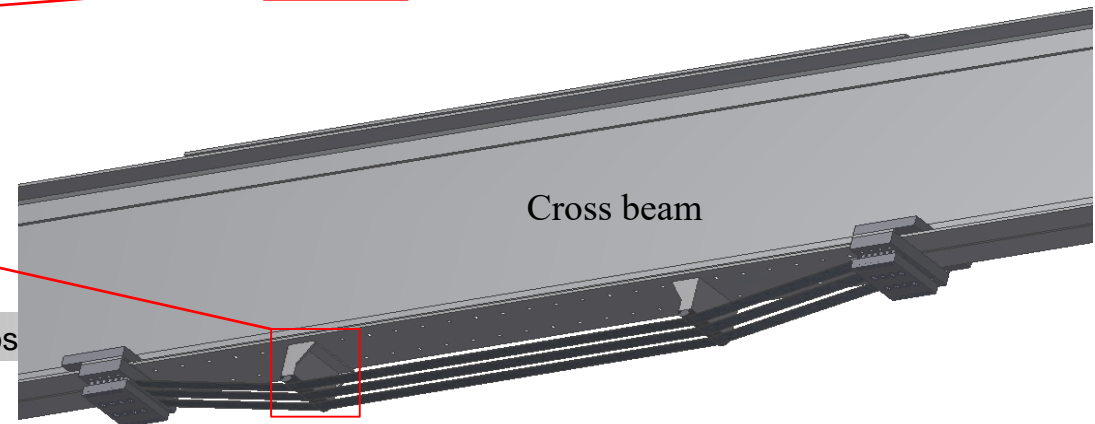
1. Applicable to unsmooth surfaces (i.g., riveted beams).
2. Fast installation (no gluing & no surface preparation).
3. Easy to prestress (no hydraulic jacks).
4. No traffic interruptions for bond curing.
5. Minimum damage (no hole, glue & grinding).
6. Adjustable prestressing level (to compensate relaxation).
7. Easy to remove.



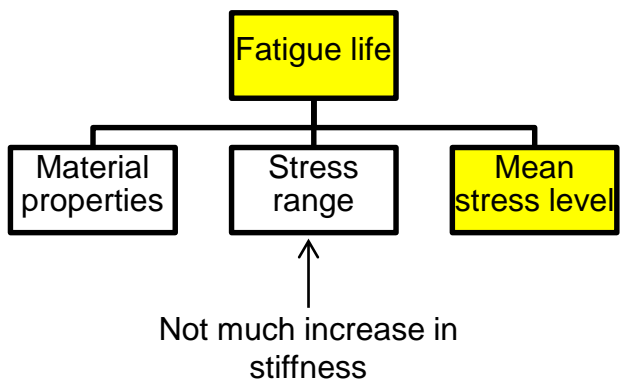
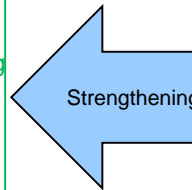
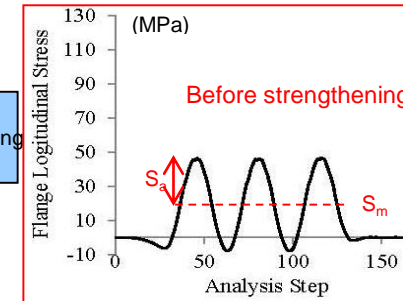
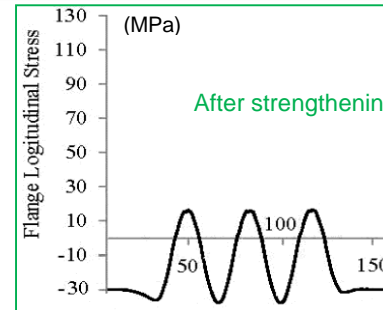
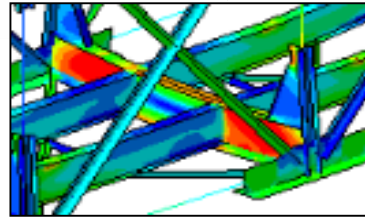
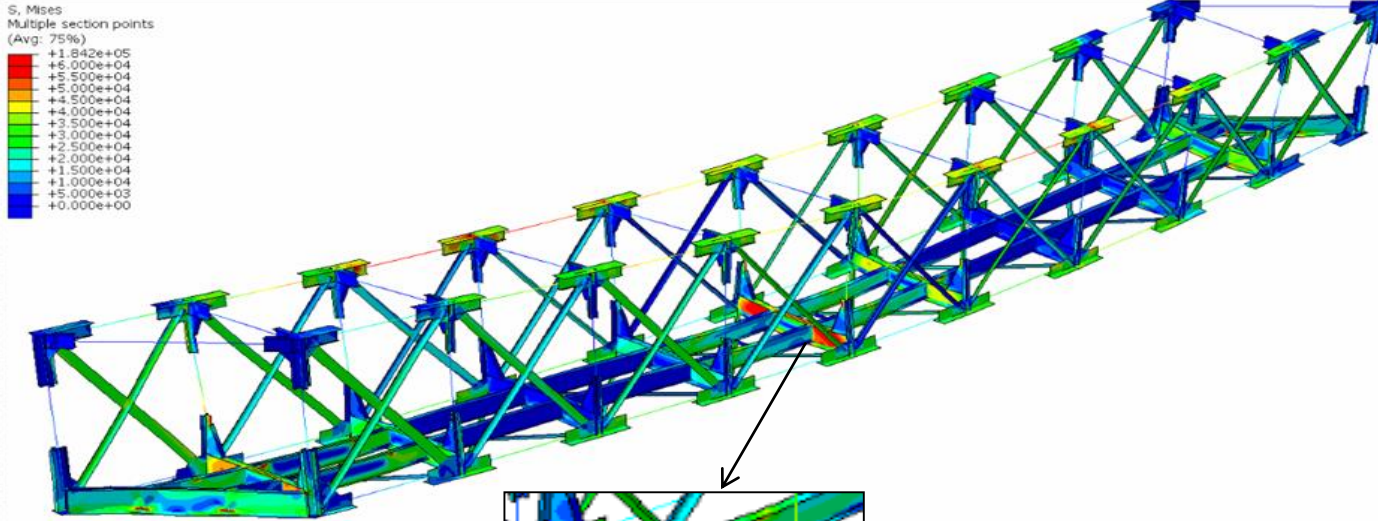
Prestressing chair (temporarily)



Column (permanent)



Fatigue Theory



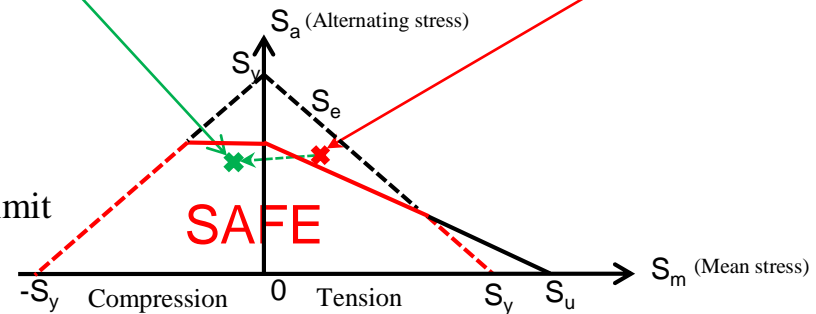
$$S_m = (\sigma_{\max} + \sigma_{\min}) / 2$$

$$S_a = (\sigma_{\max} - \sigma_{\min}) / 2$$

$$S_y = \text{yield limit}$$

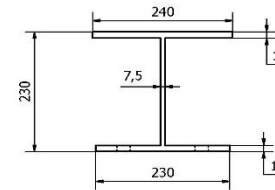
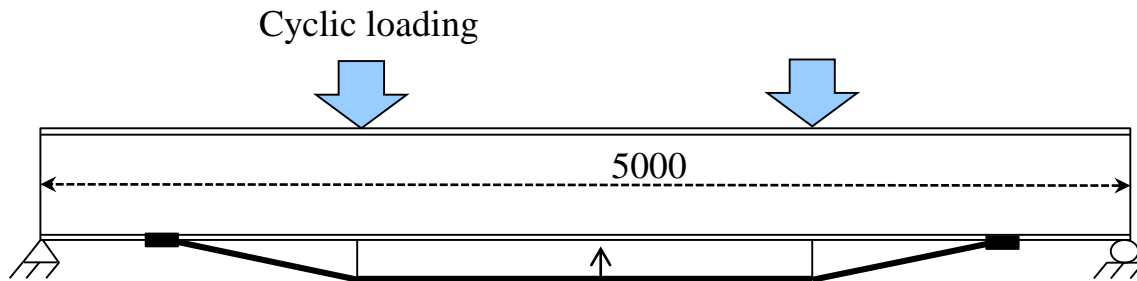
$$S_u = \text{ultimate strength}$$

$$S_e = \text{fatigue endurance limit}$$

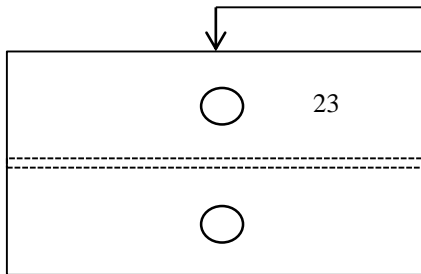


Modified Goodman Constant Life Diagram (CLD)

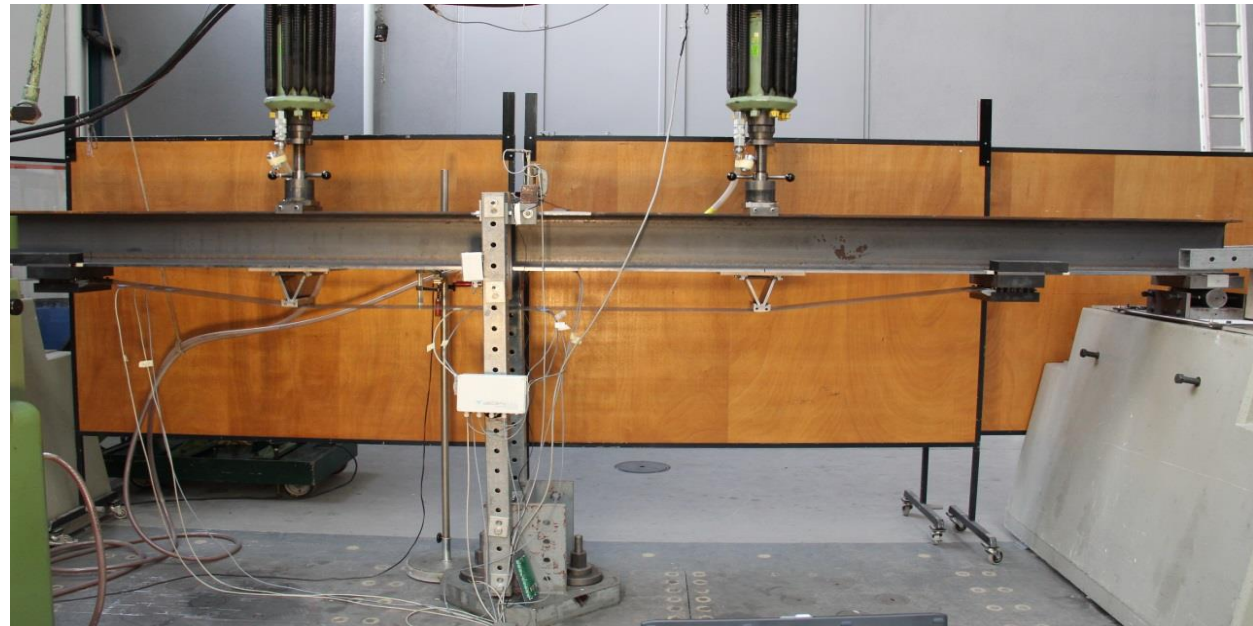
Laboratory Experiments



Dimensions in mm

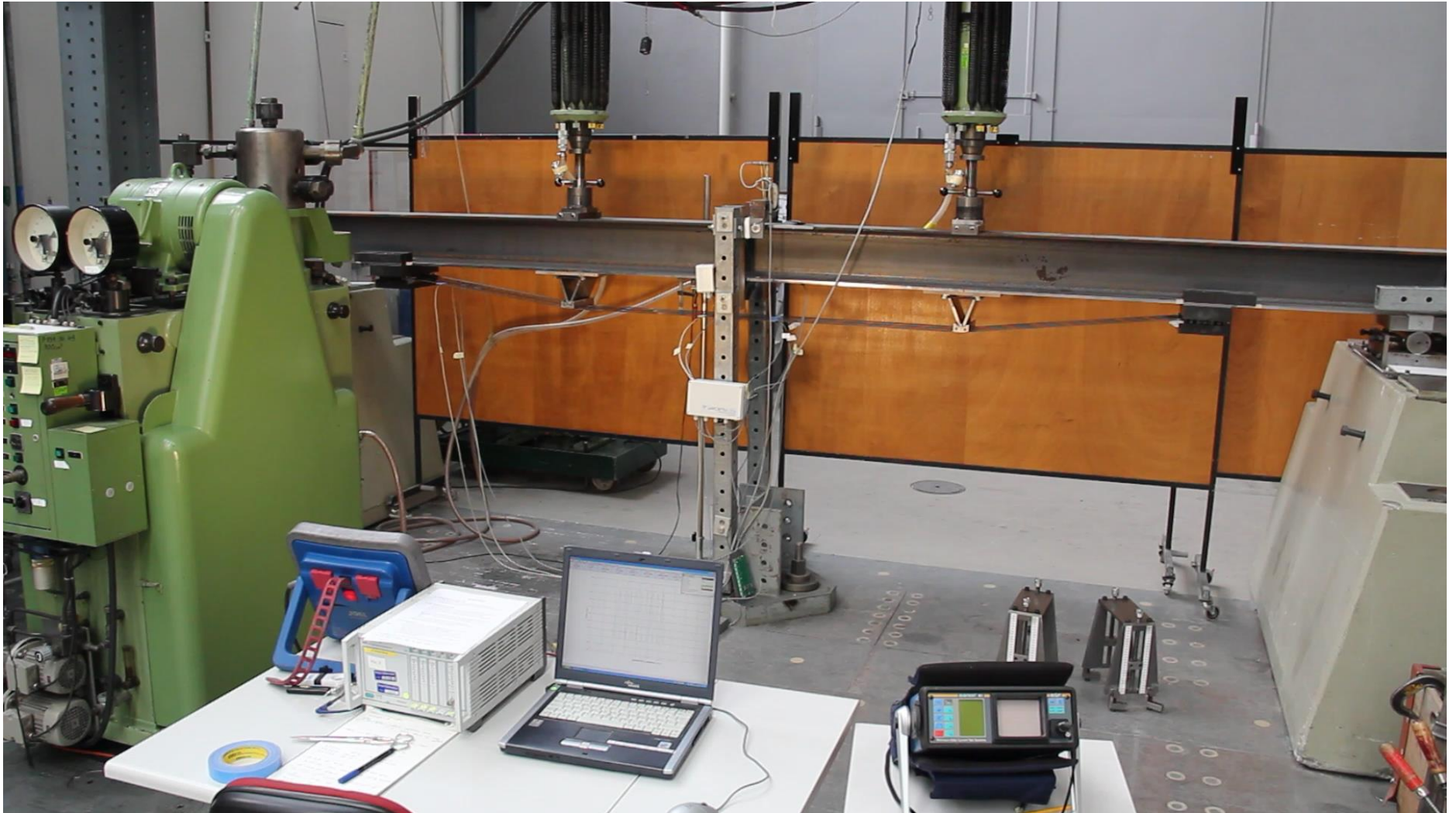


Detail of rivet holes in bottom flange of beam



Laboratory Experiments

Video



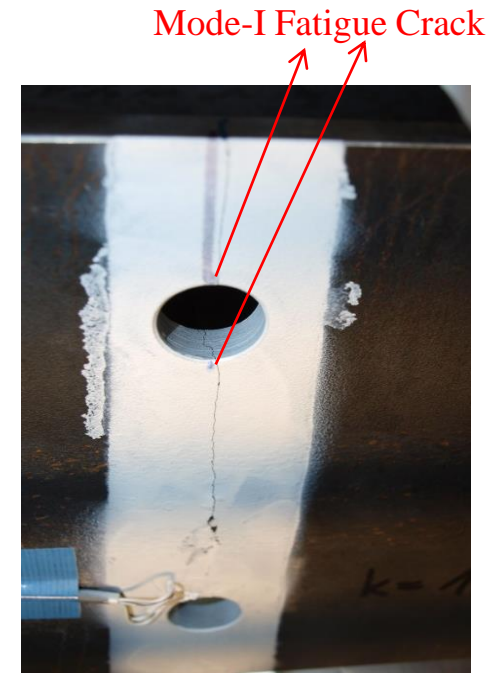
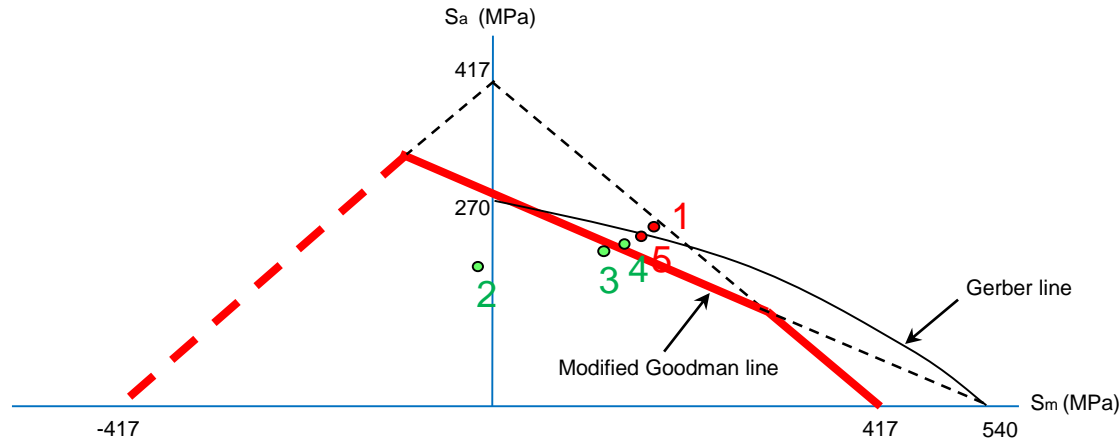
Steel Strengthening

Fibre Composites

Hossein Heydarinouri

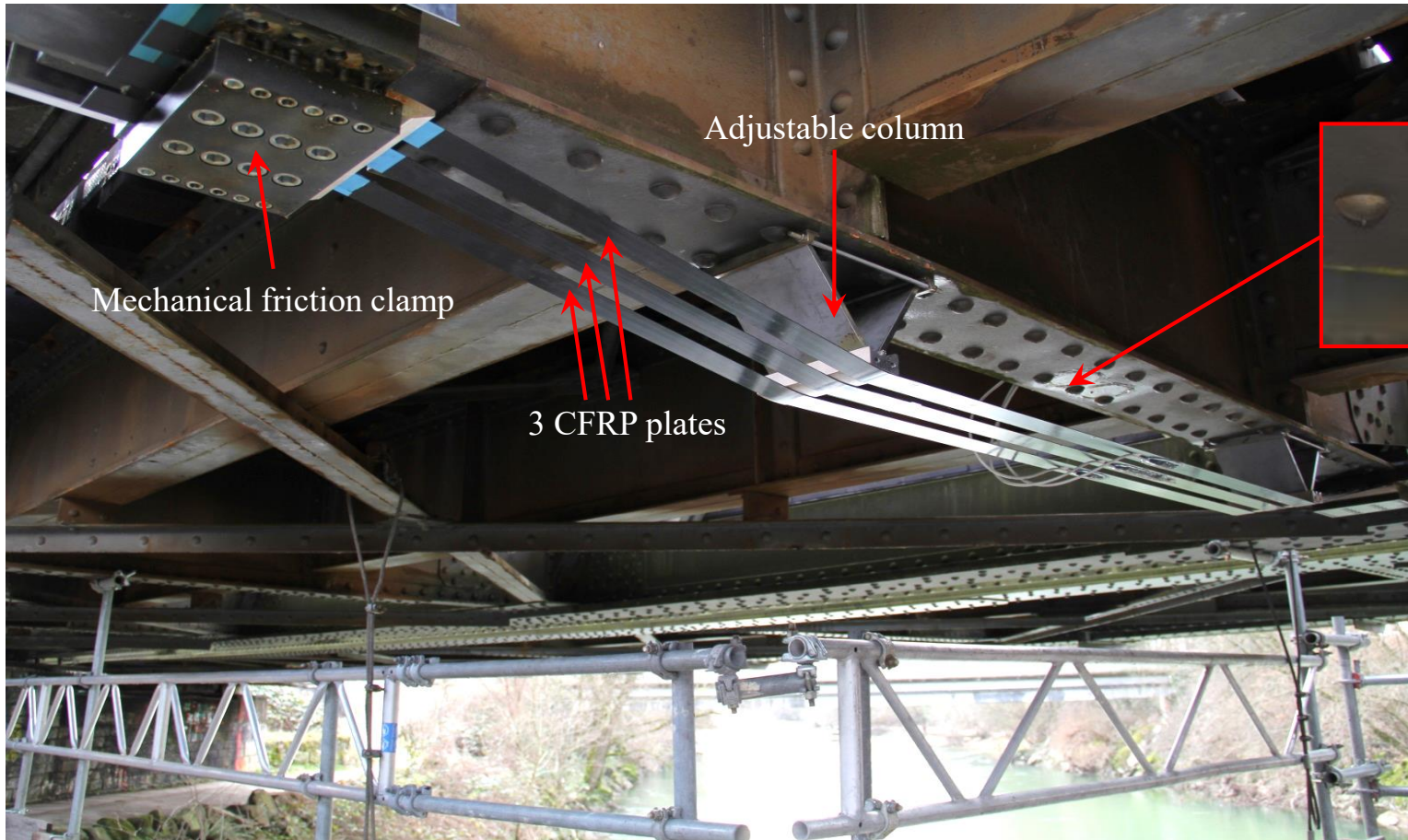
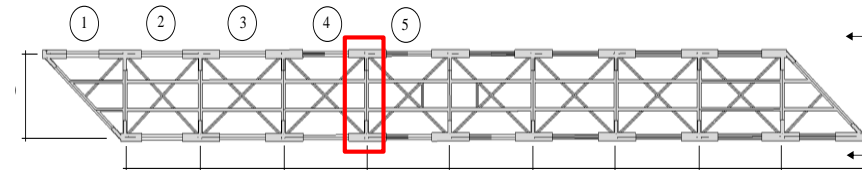
47

Laboratory Experiments

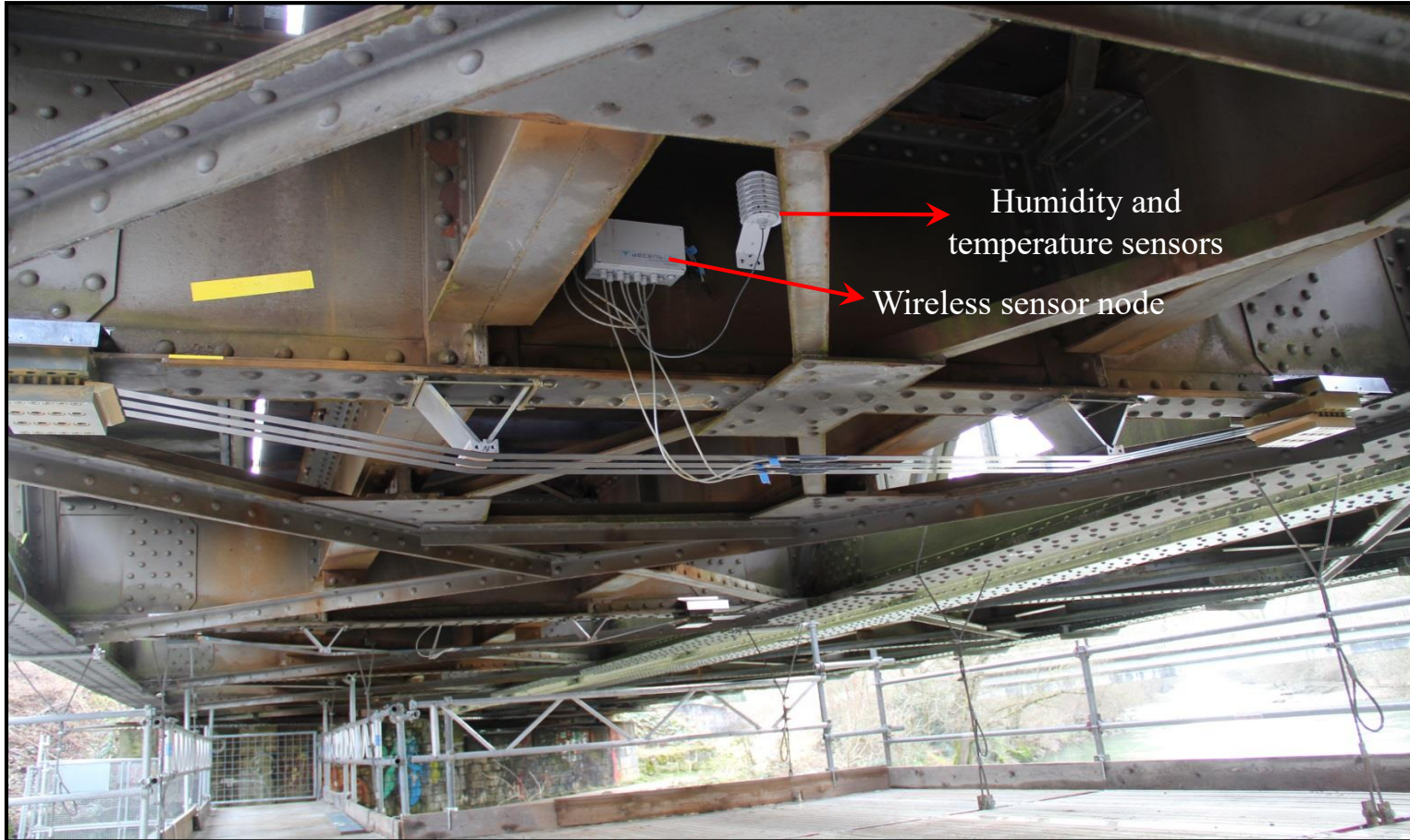
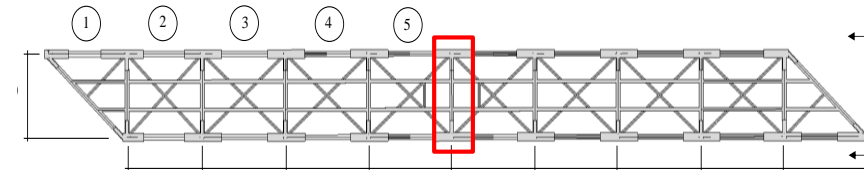


- Fatigue test 1 (beam 1), not strengthened: $F=[2.5-68]$ kN $\rightarrow N= 500'000$ cycles \rightarrow **cracked**
- Fatigue test 2 (beam 2), 30% prestressing: $F=[2.5-68]$ kN $\rightarrow \Delta N=2'000'000$ cycles \rightarrow **No crack**
- Fatigue test 3 (beam 2), 22% prestressing: $F=[2.5-68]$ kN $\rightarrow \Delta N=3'000'000$ cycles \rightarrow **No crack**
- Fatigue test 4 (beam 2), 14% prestressing: $F=[2.5-68]$ kN $\rightarrow \Delta N=3'000'000$ cycles \rightarrow **No crack**
- Fatigue test 5 (beam 2), 4% prestressing: $F=[2.5-68]$ kN $\rightarrow \Delta N=1'500'000$ cycles \rightarrow **cracked**

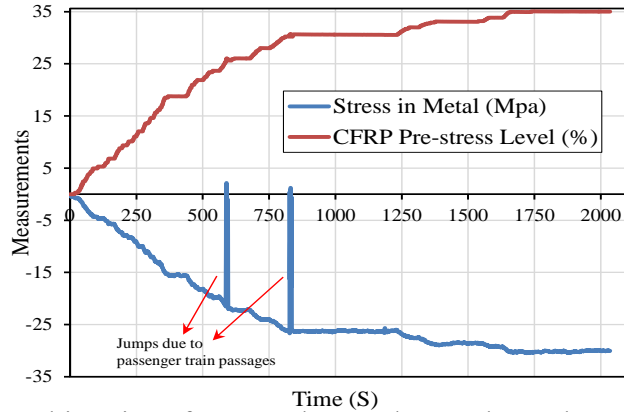
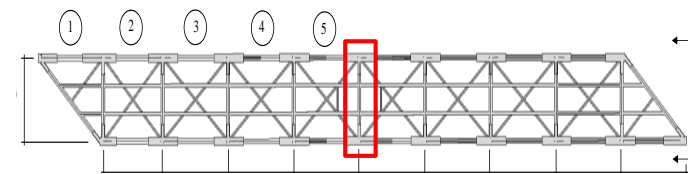
Laboratory Experiments



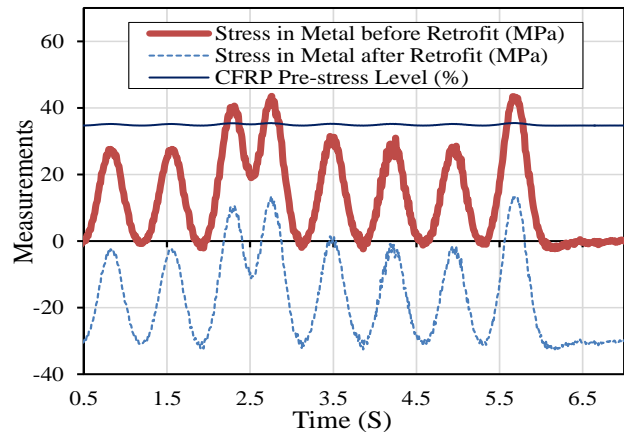
Bridge Strengthening



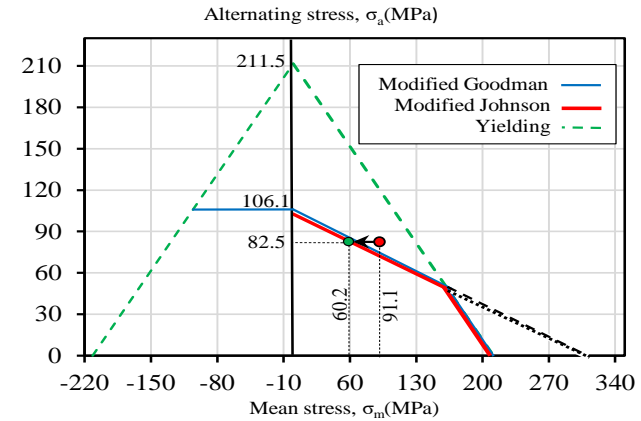
Bridge Strengthening



Stress-histories of CFRP plate and cross-beam bottom flange while pre-stressing



Stress-histories of CFRP plate and cross-beam bottom flange before & after strengthening due to S3 train



CLD presentation of shifting stresses from finite life zone to infinite life region using pre-stressed CFRP material (D4 load model)

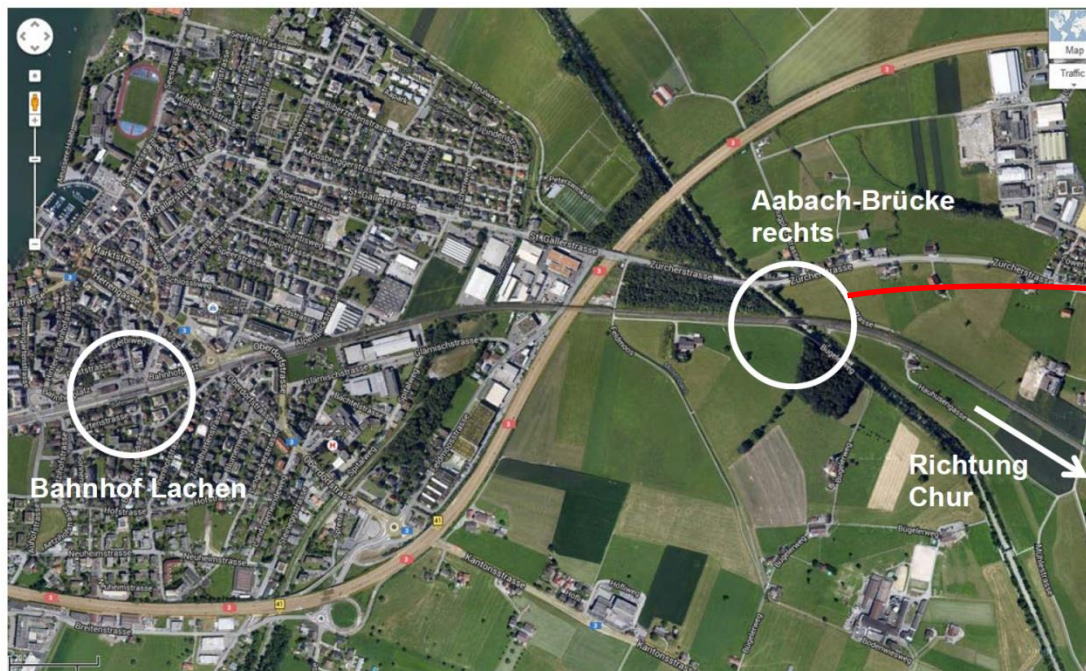


A S3 passenger train crossing Münchenstein Bridge

Case Study:
Fatigue Strengthening of Aabach Railway Bridge Connections

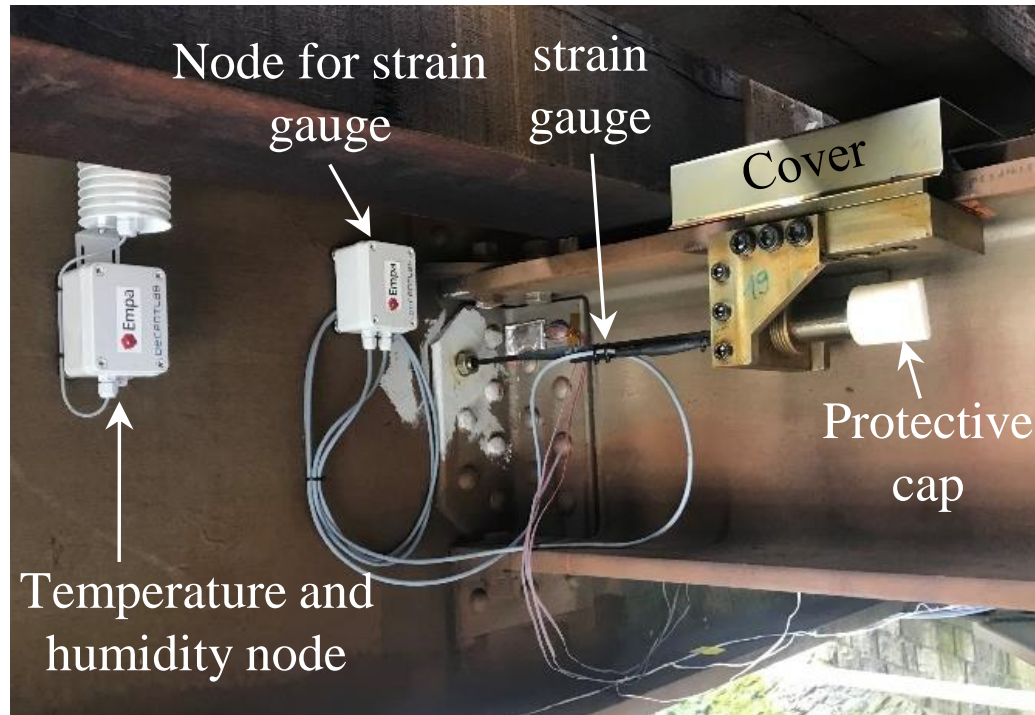
Aabach Bridge in Lachen, Switzerland

- Riveted railway bridge
- Built in 1928
- Total Length: 38.7 m
- Subjected to passenger and freight trains



Aabach Bridge in Lachen, Switzerland

Strengthening of the connections

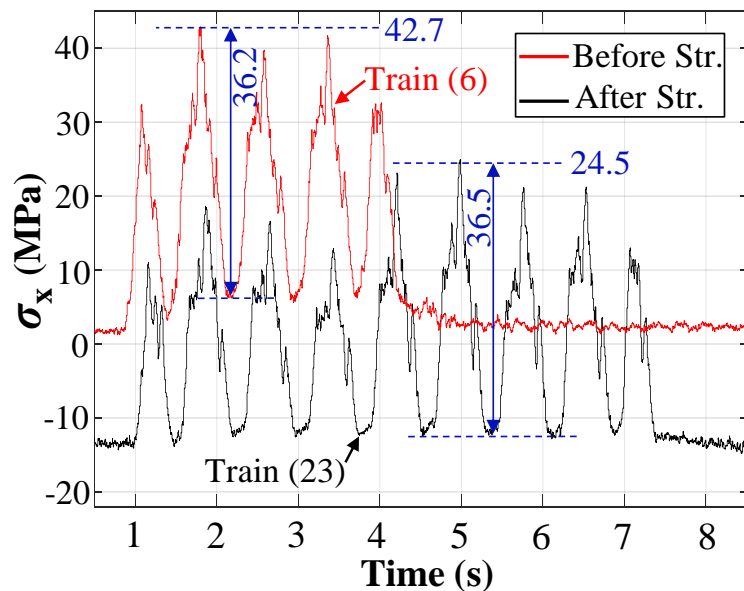


Rosette strain gauge for the short-term measurements

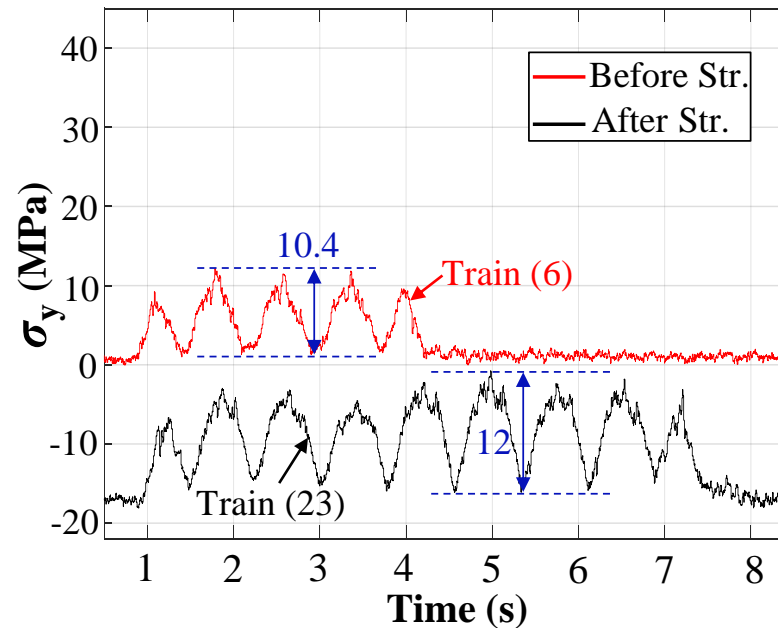
Aabach Bridge in Lachen, Switzerland

Strengthening of the connections

Strengthening effect on the stresses due to passage of **passenger trains**.



x-direction



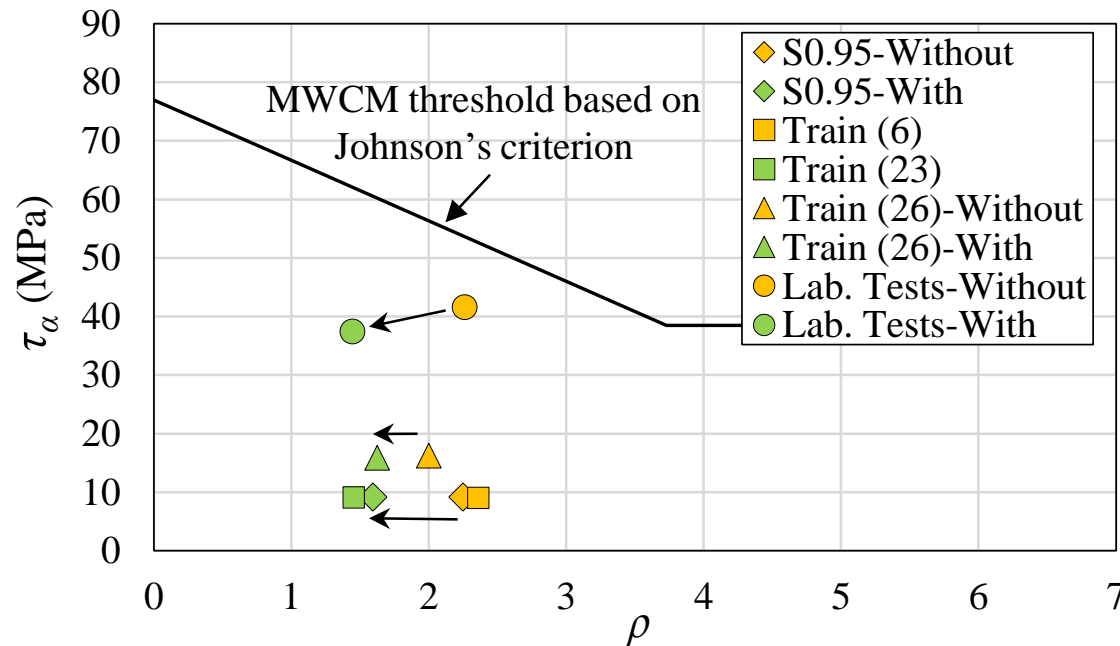
y-direction

Strengthening system reduced on only the mean stress, and not the stress range.

Aabach Bridge in Lachen, Switzerland

Strengthening of the connections

- MWCM diagram to evaluate the fatigue state before and after strengthening.



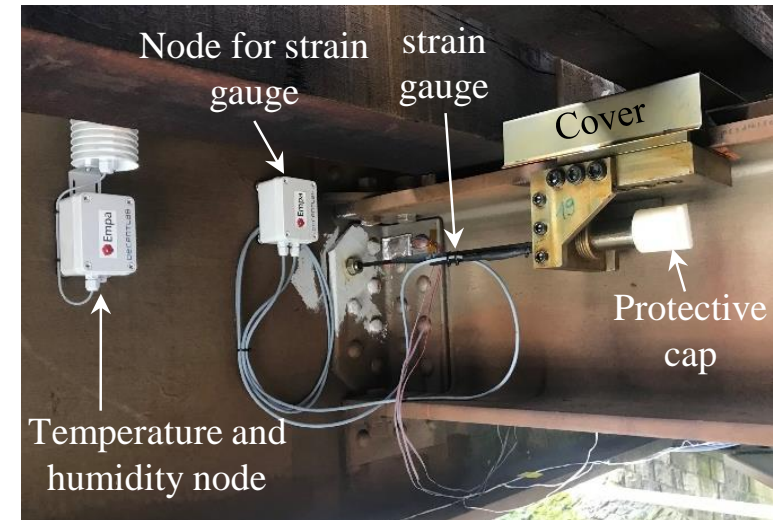
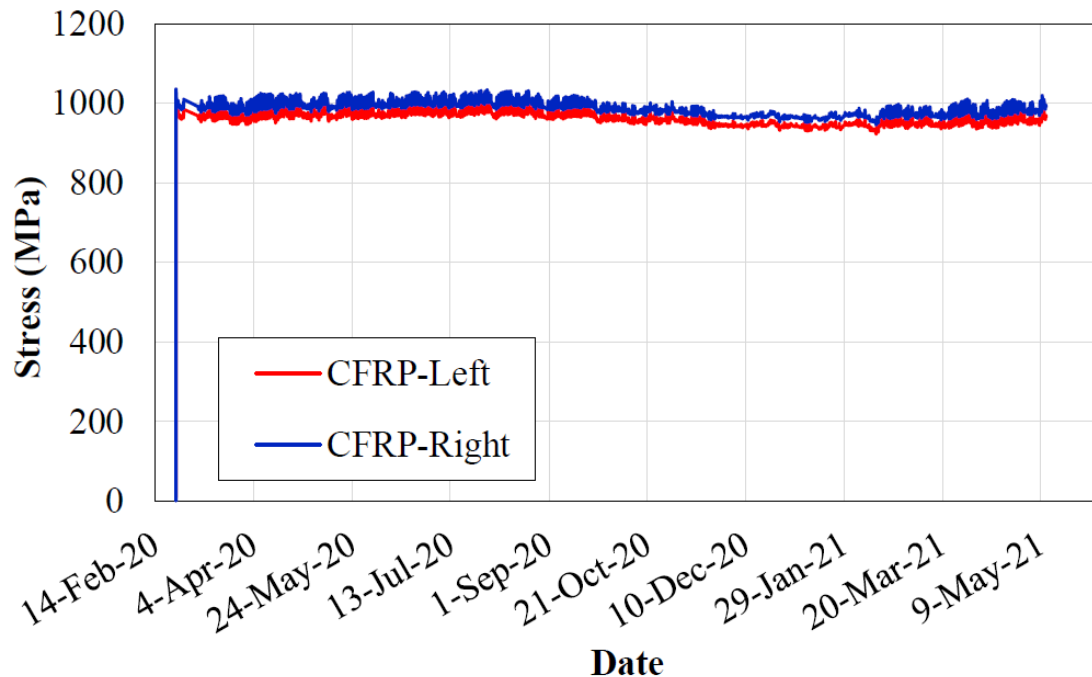
The effectiveness of the strengthening system in reducing the stresses depends on the type of the train.

Aabach Bridge in Lachen, Switzerland

Strengthening of the connections

- Long-term monitoring

Stress history of the CFRP rods



No prestressing loss occurred in the CFRP rods since the installation.

Conclusions: Prestressed vs. Non-prestressed CFRP Plates

Advantages:

- Utilization of high tensile strength of CFRP materials
- Prestressed FRPs can carry both a portion of the dead load and the additional live load carried by the structure
- Increasing yielding load
- Increasing ultimate load capacity
- Substantial increase in fatigue life
- Possible arrest of existing fatigue cracks

Conclusions: Prestressed vs. Non-prestressed CFRP Plates

Disadvantages:

- Large amount of labor work for prestressing (you can almost forget about CFRP cost).
- High interfacial shear stresses at plate ends => earlier debonding => use of mechanical anchorage system

Conclusions: Bonded vs. Un-bonded CFRP-steel Composite Systems

- **Weak point:**

The main difference between FRP–steel and FRP–concrete bonded joints is that in the former, failure will likely occur in the adhesive layer and in the latter failure is expected to occur in the concrete. Thus the weakest point in FRP-steel composite systems is the adhesive.

- **Surface preparation:**

Prior to bond application, surface of steel beam should be cleaned and all paint and anti-corrosion coating have to be removed.

- **High temperature:**

Compared to concrete, steel has a high thermal conductivity (about 50 W/mK) and has significant ability to transfer heat rapidly to the adhesive. Moreover, the rate of sunlight absorption by steel is much greater than the rate of steel electromagnetic radiation (black body radiation); therefore, steel members exposed to direct sunlight on a hot day will easily become much hotter than the ambient temperature. This effect makes the adhesive adjacent to a hot steel surface soften excessively when the service temperature of the steel substrate approaches the glass transition temperature of the adhesive.

- **Metallic riveted bridges:**

Due to the flat configuration of FRP plates, they cannot be bonded to the surface of structures that are not sufficiently smooth. Because the cover plate is riveted to the steel girders in steel-riveted bridges, for example, there is a high rivet density and the bonded FRP reinforcement system cannot be used.

- **Heritage structures:**

The components of strengthening systems for heritage structures need to be designed for easy removal when there is a need to restore the structure to its original unstrengthened construction design. In a bonded reinforcement system, FRP strengthening materials cannot be easily separated from the beam due to the applied glue.

References

- Ghafoori E., Motavalli M., Zhao X.L., Nussbaumer A., Fontana M. Fatigue design criteria for strengthening metallic beams with bonded CFRP plates. *Engineering Structures*, 2015. 101: p. 542-557.
- Ghafoori E., Motavalli M., Nussbaumer A., Herwig A., Prinz G., Fontana M. Determination of minimum CFRP pre-stress levels for fatigue crack prevention in retrofitted metallic beams. *Engineering Structures*, 2015. 84: p. 29–41.
- Ghafoori E., Motavalli M., Nussbaumer A., Herwig A., Prinz G.S., Fontana M. Design criterion for fatigue strengthening of riveted beams in a 120-year-old railway metallic bridge using pre-stressed CFRP plates. *Composites Part B*, 2015. 68: p. 1-13.
- Ghafoori E., Motavalli M. Normal, high and ultra-high modulus CFRP laminates for bonded and un-bonded strengthening of steel beams. *Materials and Design*, 2015. 67: p. 232–243.
- Ghafoori E., Motavalli M. Lateral-torsional buckling of steel I-beams retrofitted by bonded and un-bonded CFRP laminates with different pre-stress levels: experimental and numerical study. *Construction and Building Materials*, 2015. 76: p. 194–206.
- Ghafoori E., Prinz G.S., Mayor E., Nussbaumer A., Motavalli M., Herwig A., Fontana M. Finite element analysis for fatigue damage reduction in metallic riveted bridges using pre-stressed CFRP plates. *Polymers*, 2014. 6(4): p. 1096-1118.
- Ghafoori E., Motavalli M. Flexural and interfacial behavior of metallic beams strengthened by prestressed bonded plates. *Composite Structures*, 2013. 101: p. 22-34.
- Ghafoori E., Schumacher A., Motavalli M. Fatigue behavior of notched steel beams reinforced with bonded CFRP plates: Determination of prestressing level for crack arrest. *Engineering Structures*, 2012. 45: p. 270-283.
- Ghafoori E., Motavalli M., Botsis J., Herwig A., Galli M. Fatigue strengthening of damaged metallic beams using prestressed unbonded and bonded CFRP plates. *International Journal of Fatigue*, 2012. 44: p. 303-315.
- Ghafoori E., Motavalli M., Flexural and interfacial behavior of metallic beams strengthened by prestressed bonded plates, *Composite Structures*, 101 (2013), 22-34.

References

- Heydarinouri, H., Nussbaumer, A., Motavalli, M., & Ghafoori, E. (2021). Multiaxial fatigue criteria for prestressed strengthening of steel connections. *International Journal of Fatigue*, 153, 106470.
- Heydarinouri, H., Motavalli, M., Nussbaumer, A., & Ghafoori, E. (2021). Development of mechanical strengthening system for bridge connections using prestressed CFRP rods. *Journal of Structural Engineering*, 147(3), 04020351.
- Heydarinouri, H., Nussbaumer, A., Motavalli, M., & Ghafoori, E. (2021). Strengthening of steel connections in a 92-year-old railway bridge using prestressed CFRP rods: Multiaxial fatigue design criterion. *J Bridge Eng*, 26(6), 04021023.

Thank You for Your Attention!

Any Questions?